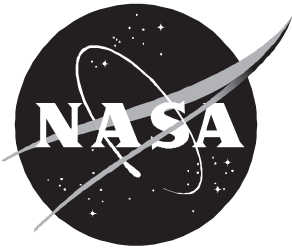




# Separation Characteristics of Generic Stores From Lee Side of an Inclined Flat Plate at Mach 6

---

*Floyd J. Wilcox, Jr.*



# Separation Characteristics of Generic Stores From Lee Side of an Inclined Flat Plate at Mach 6

---

*Floyd J. Wilcox, Jr.*  
*Langley Research Center • Hampton, Virginia*

Available electronically at the following URL address: <http://techreports.larc.nasa.gov/ltrs/ltrs.html>

Printed copies available from the following:

NASA Center for AeroSpace Information  
800 Elkridge Landing Road  
Linthicum Heights, MD 21090-2934  
(301) 621-0390

National Technical Information Service (NTIS)  
5285 Port Royal Road  
Springfield, VA 22161-2171  
(703) 487-4650

## Summary

An experimental investigation was conducted to determine the aerodynamic characteristics of two store shapes as they were separated away from the lee side of a flat plate at Mach 6. The flat plate was inclined at  $15^\circ$  to the free-stream flow to provide a separated flow region through which the stores were traversed. Flow visualization data (oil flow and schlieren photographs) showed that the flat plate lee-side flow field actually consisted of a separated flow region, a separation shock wave, an expansion fan region, and a weak shock wave from the leading edge of the plate. The two store test shapes were a cone cylinder and a roof delta. Force and moment data for the stores were obtained as they were traversed in 0.5-in. increments from a position near the flat plate surface into the free-stream flow. The angle of attack of the stores was held constant at either  $0^\circ$  or  $15^\circ$  as they were separated away from the plate.

The results of this investigation showed that both the cone cylinder and the roof delta had unfavorable store separation characteristics (i.e., a nose-down pitching moment and a negative normal force) at an angle of attack of  $0^\circ$ , which would tend to force the store back into the flat plate. At an angle of attack of  $15^\circ$ , the cone cylinder store had favorable separation characteristics (i.e., a nose-up pitching moment and a positive normal force), which would tend to force the store away from the flat plate. However, at an angle of attack of  $15^\circ$  and small separation distances, the roof delta had indeterminate store separation characteristics, which were a consequence of the store normal force and pitching moment alternating between small positive and negative values as the separation distance increased. However, at greater store separation distances, the roof delta had favorable store separation characteristics. The store separation results for the cone cylinder and roof delta were caused by the local flow inclination relative to the stores as they were traversed away from the flat plate through the separated flow region, separation shock wave, expansion fan region, leading-edge shock wave, and then into the free-stream flow.

## Introduction

One method of improving the survivability of a military aircraft in modern battlefield environments is to increase its speed and thus decrease the time of aircraft exposure to hostile situations. Although this increase in speed can improve the aircraft survivability, it can create problems when releasing stores from the aircraft. For example, references 1–5 have shown that stores released at supersonic speeds from certain weapons bay configurations can have adverse separation characteristics that cause stores to pitch up into the parent launch vehicle.

(This store separation motion is primarily caused by the aerodynamics of the weapons bay.) Recently, the feasibility of carrying and releasing stores from vehicles at hypersonic speeds has become an important issue. (See refs. 6–8.) However, conventional store carriage (i.e., carrying stores underneath an aircraft in either a weapons bay or on the surface) cannot be used with currently proposed hypersonic vehicles because propulsion systems of these vehicles are integrated across the entire bottom surface of the aircraft. Hence, the studies in references 6 and 7 have primarily focused on methods of carriage and release of stores from either the aft end or the top surface of the aircraft. In addition to avoiding interference with the aircraft propulsion system, these store carriage methods have the potential to reduce both the aircraft radar cross-section signature and the installed store drag; the stores are shielded from the free-stream flow either by internal carriage or by external carriage in the separated flow region on the top surface of the aircraft. For internal carriage, the stores would be carried in tubes located in the aft end of the parent launch vehicle and released through its wake. (See ref. 7.) For external carriage, the stores would be mounted on the top surface of the aircraft and released through the separated flow region on the lee side of the aircraft. Some results have been computed for external carriage release and are presented in reference 6. However, little experimental data are available in the literature for aerodynamic characteristics of a store as it is separated from the lee side of a vehicle and moved into the free-stream flow at hypersonic speeds. Most available experimental data deal with the separation of two equally or nearly equally sized bodies (e.g., the Space Shuttle Orbiter and external tank) rather than of a large parent launch aircraft and a relatively small store. Therefore, an experimental investigation was conducted to determine the aerodynamic characteristics of a store as it is separated from the lee side of a vehicle and moved into the free-stream flow.

Wind tunnel tests were conducted by representing the parent launch aircraft with a flat plate that was inclined at  $15^\circ$  to the free-stream flow at Mach 6. The incidence angle of  $15^\circ$  was high enough to provide a separated flow region over the flat plate without causing wind tunnel blockage. The flat plate simplifies the overall flow field so that the separation characteristics of the store could be measured in a less-complicated two-dimensional flow field rather than in the three-dimensional flow field of an actual aircraft. In addition, the flat plate permitted the use of larger store models and balances than could be used with an actual aircraft model; the model would have been sized for a small hypersonic wind tunnel test section, and the resulting stores would have been too small for existing balances. Forces and moments on each store were measured at

discrete heights above the flat plate surface as the store was vertically traversed through the lee-side flow field and into the free-stream flow. The test stores were a cone cylinder and a roof delta. The angle of attack of the stores was held constant at either  $0^\circ$  or  $15^\circ$  as the stores were traversed away from the flat plate.

## Symbols

Aerodynamic force and moment coefficient data are presented in the store body-axis coordinate system. The moment reference centers of the cone cylinder and roof delta are located 3.50 in. and 4.58 in., respectively, aft of the model nose. (See fig. 2.)

$A$	reference area, in <sup>2</sup> (fig. 2)
$C_A$	axial-force coefficient, $\frac{\text{Drag force}}{qA}$
$C_m$	pitching-moment coefficient, $\frac{\text{Pitching moment}}{qAl}$
$C_N$	normal-force coefficient, $\frac{\text{Normal force}}{qA}$
$h$	store separation distance, in. (fig. 3)
$l$	reference length, in. (fig. 2)
$M$	free-stream Mach number
$p_0$	free-stream stagnation pressure, psia
$q$	free-stream dynamic pressure, psia
$Re$	free-stream unit Reynolds number, per ft
$T_0$	free-stream stagnation temperature, $^\circ\text{F}$
$\alpha$	angle of attack, deg

## Experimental Methods

### Model Description

A flat plate at an angle of attack of  $15^\circ$  was mounted on the tunnel floor with two support struts as shown in figure 1. Both support struts had wedge-shaped leading edges with an included angle of  $30^\circ$  and were located sufficiently downstream of the plate leading edge to prevent interference with the lee-side flow field. The plate was 11.5 in. wide by 21 in. long with a leading-edge wedge angle of  $10^\circ$  so that an attached shock wave could be maintained at the leading edge. The plate trailing edge had a wedge angle of  $15^\circ$  to aid in turning the windward surface flow parallel with the free-stream flow without separating and causing disturbances in the flat plate lee-side flow field.

The stores used in this investigation consisted of a cone cylinder and a roof delta as shown in figure 2. Both stores were originally designed to be 7.00 in. long; however, a machining error occurred during the fabrication of the roof delta and its overall length was reduced by 0.13 in. The stores were designed to be as small as possible to fit an existing water-cooled balance and still be immersed in the flat plate separated flow field at the lowest store separation height. Another strut located 6.0 in. aft of the plate trailing edge supported the sting holder, sting, balance, and store model. (See fig. 1(b).) Because of sting bending stress considerations, the sting diameter was increased near the sting holder; however, a constant minimum sting diameter was maintained for at least three-store diameters from the base of the store to minimize sting effect on the measured forces and moments. The strut extended through the tunnel floor plate and was supported with a bracket. The leading-edge wedge of both the strut and bracket had an included angle of  $40^\circ$ . The strut length above the flat plate was manually adjusted in 0.5-in. vertical increments with a shoulder bolt in the support bracket. Two different struts were used to hold the stores at an angle of attack of either  $0^\circ$  or  $15^\circ$ . The total vertical movements of the struts at angles of attack of  $0^\circ$  and  $15^\circ$  were 7.5 in. and 9.0 in., respectively; the difference resulted from the requirement that the entire store be located in the free-stream flow at the highest vertical position. Figure 3 shows the location of the stores relative to the flat plate at the lowest store separation height and the sign convention used for the store separation height  $h$ . The nose of each store was located 11.38 in. from the plate leading edge (measured along the flat plate surface) at the lowest separation height.

### Wind Tunnel

The tests were conducted in the Langley 20-Inch Mach 6 Tunnel. (See fig. 4.) This tunnel is a blow-down facility that has a fixed-geometry two-dimensional nozzle with parallel sidewalls and a test section that is 20 in. wide by 20.5 in. high. High-pressure air is supplied to the tunnel from a storage bottle field and is discharged into a 60-ft-diameter vacuum sphere which can be connected to a 100-ft- and/or a 40-ft-diameter vacuum sphere to obtain additional run time. The supply air is heated with an electrical resistance heater to prevent air liquefaction. The tunnel has a stagnation pressure range of 45 to 515 psia and a stagnation temperature range of  $290^\circ$  to  $540^\circ\text{F}$ . The tunnel is equipped with a model injection mechanism to reduce starting and stopping loads on the model. A more detailed description and the calibration of the facility are presented in the appendix of reference 9.

## Test Conditions

The tests were conducted at the following average test conditions:

$$M = 6$$

$$p_0 = 100 \text{ psia}$$

$$T_0 = 360^\circ\text{F}$$

$$q = 1.60 \text{ psia}$$

$$Re = 2.06 \times 10^6 \text{ per foot}$$

The high-pressure air used in the facility was sufficiently dried and heated to minimize water condensation and prevent air liquefaction at the test conditions. Boundary layer transition grit was not applied to the leading edges of either the flat plate or the stores.

## Measurements and Data

Forces and moments on the stores were measured with a six-component electrical strain gage balance. The balance was water cooled to minimize thermal gradients within the balance from aerodynamic heating of the store models. Two thermocouples were mounted on the forward and aft sections of the balance to monitor thermal gradients during each test run. Although all six balance components were measured, only longitudinal force and moment data are presented in this report because the symmetry of the models resulted in insignificant lateral forces and moments.

A typical test run began with the model retracted in the tunnel injection pit. (See fig. 4.) After tunnel flow was established, the model was injected into the flow, and the tunnel stagnation pressure and temperature were increased to the required test conditions and allowed to stabilize. Typically, test data were acquired every 10 sec for approximately 2 to 3 min to determine when the store base and chamber pressures settled completely. When the data acquisition process was completed, the model was retracted into the injection pit, and the tunnel flow was stopped.

Both base and balance chamber pressures were measured on the roof delta. Because a chamfer on the rear of the cone cylinder eliminated the base area entirely, only balance chamber pressures were measured on the cone cylinder. Chamber pressures were measured on each store with two tubes located in the vicinity of the balance. Base pressures were measured at two locations (fig. 5) on the roof delta with tubes that were routed along the sting and bent so that they were perpendicular to and in close proximity of the base. The base pressures and chamber pressure data were averaged separately and used to correct the force and moment data to a condition

of free-stream static pressure acting over the appropriate base and chamber areas. (See fig. 5.) The magnitude of these corrections on the axial-force coefficient for both stores are shown in figure 6.

Schlieren photographs of the flat plate model were taken during this test. The schlieren system knife-edge was oriented parallel to the free-stream flow to highlight density gradients in the vertical direction. For this knife-edge orientation, increasing density gradients in the upward direction appear as white areas in the photographs. The appendix presents schlieren photographs (figs. A1–A4) of both stores at all separation heights.

Oil flow photographs were taken to document the flow field on the lee side of the flat plate. The technique used for the oil flows consisted of painting the flat plate black and wiping the surface with a lint-free rag soaked with oil having a kinematic viscosity of 50 centistokes (dimethylpolysiloxane silicone fluid) so that a thin base coat of oil covered the plate. Individual drops of oil with a kinematic viscosity of 50 centistokes mixed with white acrylic oil-based paint were applied on the flat plate with a hypodermic needle and syringe in a grid pattern with a spacing of approximately 0.5 in. between oil drops for the first 7.0 in. of the plate and 1.0 in. between oil drops for the remaining length of the plate. The procedure used for the oil flow tests differed from that used for the force and moment tests; the model remained in the injection pit out of the tunnel flow until the stagnation pressure and temperature stabilized at the required test conditions. The model was then injected into the flow for approximately 15 to 20 sec before being retracted. Photographs were then taken of the resulting oil flow streak patterns.

The uncertainty of the force and moment data was determined from the quoted accuracy in table I for the balance, which is  $\pm 0.5$  percent of the full-scale output of each balance component. The accuracy of each balance component in pounds or inch-pounds was reduced to coefficient form and resulted in the approximate coefficient uncertainties in table II. These uncertainty values do not account for all possible sources of experimental error but do indicate an order of magnitude of the uncertainty of the coefficient data. Because the purpose of this test was to determine major trends in the data and not to provide absolute coefficient values, a more extensive uncertainty analysis was not performed. The experimental data from this test are tabulated in table III.

## Discussion of Results

### Flat Plate Flow Field

Before store separation data were obtained, flow visualization tests were conducted to document the lee-side flat plate flow field without stores present. Oil flow

and schlieren photographs of the flat plate are shown in figure 7. The oil flow photograph shows that the flow expanded around the plate leading edge and remained attached to the plate surface for approximately 5 in. downstream of the leading edge. The oil flow drops along the edges of the plate show a slight outward flow, which is probably caused by edge vortices. The effect of these edge vortices appears to be limited to the outer 1.5 in. of the plate edges. A recirculation region occurs approximately over the last 2 in. of the flat plate. Because the stores were located on the flat plate centerline and were more than 2 in. from the plate trailing edge, the effects of the edge vortices and the trailing-edge recirculation region on the store separation characteristics were probably minimal.

The schlieren photograph of the flat plate flow field shown in figure 7(b) also indicated that the flow separates from the flat plate approximately 5 in. downstream of the leading edge. The dark line emanating from the separation point is a shear layer that delineates the separated flow region. A separation shock wave is indicated by the white line emanating from the separation point. A weak shock wave is attached to the flat plate leading edge and is caused by a combination of the plate leading-edge bluntness and the initial boundary layer growth on the plate. With the oil flow and schlieren photographs as guides, a sketch of the flat plate flow field was created and is shown in figure 8. Because the flow expands around the plate leading edge and remains attached to the plate, the maximum Mach number based on inviscid isentropic expansion on the lee side of the plate is approximately 9.2. Figures 9 and 10 include sketches of the stores at all of the separation test heights superimposed on the flat plate flow field sketch. These sketches clearly indicate that none of the stores were completely submerged in the separated flow region even at the lowest store separation height, although at  $\alpha = 15^\circ$ , the stores are nearly submerged. Examination of the schlieren photographs (figs. A1–A4) in the appendix indicate that the interaction of the store with the flow field generally causes the separation shock wave to nearly disappear when the stores are at the lowest or next to lowest separation height. Although the flow field sketches in figures 9(a), 9(b), 10(a), and 10(b) do not show this effect, they do show the salient features of the flow field, can be of considerable assistance in interpreting the store separation data, and are used as the basis of the data analysis which follows.

### Store Separation Characteristics

**Cone cylinder.** The store separation characteristics of the cone cylinder are shown in figure 9(c). At  $\alpha = 0^\circ$ , the normal force remains slightly negative for the entire

store separation distance until the store was virtually in the free-stream flow at  $h = 5.89$  in. (See fig. 9(a).) This negative normal force is caused by the local downward flow angularity relative to the store centerline, which is a result of the expansion fan at the plate leading edge. As the store was moved closer to the free-stream flow, this flow angularity decreases, and the normal force on the store increases toward zero. At the lowest separation height, the pitching moment is near zero, as would have been expected, because the store was partially submerged in the low- $q$  separated flow region. As the store height was increased to  $h = 0.89$  in., a significant nose-down pitching moment occurs, which is caused by a larger portion of the store nose being out of the separated flow region. At  $h = 2.39$  in., the store was entirely in the expansion fan region, and the pitching moment becomes less negative as  $h$  increases because the flow angularity decreases. Pitching moment becomes positive as the store moved into the free-stream flow at  $h = 5.39$  in. At this position, the store nose was partially in the free-stream flow, and the store tail was in the expansion fan region (local downward flow angularity), which causes the positive pitching moment. As  $h$  increased, the store moved completely into the free-stream flow;  $C_m$  decreases and approaches zero. Overall, these data for  $\alpha = 0^\circ$  indicate that the cone cylinder has unfavorable store separation characteristics (i.e., negative normal force and pitching moment), which would tend to force the store back into the flat plate. The primary factor influencing the store separation characteristics appears to be the flow angularity relative to the store as the store traverses the various flat plate flow fields.

The data for the cone cylinder at  $\alpha = 15^\circ$  are significantly different from the data at  $\alpha = 0^\circ$ . At the lowest separation height ( $h = 0.92$  in.), the store was almost completely submerged in the separated flow region and  $C_N$  is essentially zero. Normal force becomes positive and remains nearly constant as the store traversed the separation shock wave region ( $1.92 \text{ in.} \leq h < 3.42 \text{ in.}$ ). As  $h$  continued to increase,  $C_N$  steadily increases and then levels out as the store moved into the free-stream flow. Again, this behavior is caused by the change in local flow angularity relative to the store as it traversed the expansion fan region and moved into the free-stream flow.

The store pitching moment increases from slightly negative to positive as the store moved from the separated flow region and partially through the separation shock wave. At  $h = 2.42$  in.,  $C_m$  decreases sharply but still remains positive. At this position, the store nose was in the expansion fan region, and a portion of the tail had moved from the separated flow region into the separated shock region. The local flow angle relative to the store centerline at the tail was greater than that over the nose

because of the flow turning caused by the separation shock wave. This flow angularity tends to pitch the tail of the store upward and thus decreases the overall store pitching moment. Pitching moment increases steadily from  $h = 2.92$  in. to  $5.92$  in. where the store nose was almost completely in the free-stream flow. As the store moved farther into the free-stream flow,  $C_m$  decreases and then levels off. This characteristic is caused by the increase in the local flow angularity relative to the store centerline over the aft part of the store as it moved into the free-stream flow from the expansion fan region. In general, the cone cylinder at  $\alpha = 15^\circ$  has favorable separation characteristics (i.e., positive normal force and pitching moment), which would tend to force the store away from the flat plate.

**Roof delta.** The store separation characteristics of the roof delta are shown in figure 10(c). At  $\alpha = 0^\circ$  and the lowest separation height, only the store nose was in the separated flow region. At this position, the store normal force is negative and decreases slightly as  $h$  increased and the store moved into the expansion fan region. Normal force reaches a minimum at  $h = 4.40$  in., which is the greatest value of  $h$  where the store was completely in the expansion fan region. As the store moved into the free-stream flow,  $C_N$  increases slightly before leveling off. The store pitching moment remains near zero but slightly positive for  $h \leq 5.90$  in. except for  $h = 0.90$  in. where  $C_m$  is slightly negative. For  $h > 6.40$  in., the flow field sketch (fig. 10(a)) indicates that the store should be completely in the free-stream flow; however,  $C_m$  varies between negative and positive values in this region. Schlieren photographs at these separation heights show no disturbances that would interfere with the store and the cause of the  $C_m$  variation in this region is unknown. Overall, these data show that the store has adverse separation characteristics (i.e., essentially zero pitching moment and a negative normal force), which would tend to force the store back into the plate as was the case for the cone cylinder store at  $\alpha = 0^\circ$ .

The roof delta data at  $\alpha = 15^\circ$  is significantly different from the data at  $\alpha = 0^\circ$ . Normal force remains near zero for  $0.40 \text{ in.} \leq h \leq 3.90 \text{ in.}$  as the store moved through the separated flow field, through the separation shock wave region, and into the expansion fan region. As  $h$  increased,  $C_N$  steadily increases and levels off as the store moved completely into the free-stream flow. Pitching moment alternates between small positive and negative values as the store traversed the separated flow region and the separation shock wave ( $0.40 \text{ in.} \leq h \leq 2.40 \text{ in.}$ ). For  $h \geq 3.40 \text{ in.}$ ,  $C_m$  remains positive and increases steadily up to a maximum at  $h = 5.90 \text{ in.}$  At this point, the store nose was in the free-

stream flow, and the tail was in the expansion fan region. As the store moved farther into the free-stream flow,  $C_m$  decreases sharply. This decrease is probably caused by the variation of the flow angularity relative to the roof delta as it moved into the free-stream flow as did the cone cylinder. In general, the roof delta store at  $\alpha = 15^\circ$  has indeterminate separation characteristics for  $h$  less than approximately 4 in. because the store normal force and pitching moment alternate between small positive and negative values in this region. (Here, *indeterminate separation characteristics* means that the actual dynamic store separation characteristics cannot be ascertained from the static test data.) However, at greater values of  $h$ , the store has favorable separation characteristics as the store pitching moment and normal force become positive.

## Conclusions

A wind tunnel investigation was conducted to determine the store separation characteristics of two different store shapes from the lee side of a flat plate at Mach 6. The flat plate represented a parent launch aircraft and was inclined  $15^\circ$  to the free-stream flow. The store shapes consisted of a cone cylinder and a roof delta. The stores were traversed away from the flat plate at a constant angle of attack of either  $0^\circ$  or  $15^\circ$ . Force and moment data were obtained at discrete separation distances from the flat plate surface. The following are the major conclusions of this investigation:

1. Both the cone cylinder and roof delta stores had unfavorable store separation characteristics (i.e., negative normal force and pitching moment) at an angle of attack of  $0^\circ$ , which would tend to force the store back into the flat plate.
2. At an angle of attack of  $15^\circ$ , the cone cylinder had favorable store separation characteristics (i.e., positive normal force and pitching moment), which would tend to force the store away from the flat plate. In contrast, at an angle of attack of  $15^\circ$  and separation heights of less than approximately 4 in., the roof delta store had indeterminate store separation characteristics because the store normal force and pitching moment alternate between small positive and negative values in this region. However, as the store separation height increased, the store had favorable separation characteristics.
3. The flat plate lee-side flow field consisted of a separated flow region, a separation shock wave, an expansion fan region, and a weak shock wave from the flat plate leading edge. The primary factor affecting the store separation characteristics was the local flow angularity relative to the store as it traversed the flat plate lee-side flow field.



## References

1. Rainey, Robert W.: *A Wind-Tunnel Investigation of Bomb Release at a Mach Number of 1.62*. NACA RM L53L29, 1954.
2. Stallings, Robert L., Jr.: Store Separation From Cavities at Supersonic Flight Speeds. *J. Spacecr. & Rockets*, vol. 20, no. 2, Mar.–Apr. 1983, pp. 129–132.
3. Blair, A. B., Jr.; and Stallings, R. L., Jr.: Cavity Door Effects on Aerodynamic Loads of Stores Separating From Cavities. *J. Aircr.*, vol. 26, July 1989, pp. 615–620.
4. Stallings, Robert L., Jr.; and Forrest, Dana K.: *Separation Characteristics of Internally Carried Stores at Supersonic Speeds*. NASA TP-2993, 1990.
5. Stallings, Robert L., Jr.; Wilcox, Floyd J., Jr.; and Forrest, Dana K.: *Measurements of Forces, Moments, and Pressures on a Generic Store Separating From a Box Cavity at Supersonic Speeds*. NASA TP-3110, 1991.
6. Newman, Gary; Fulcher, Karen; Ray, Robert; and Pinney, Mark: On the Aerodynamics/Dynamics of Store Separation From Hypersonic Aircraft. AIAA-92-2722, June 1992.
7. Butler, G.; King, D.; Abate, G.; and Stephens, M.: Ballistic Range Tests of Store Separation at Supersonic to Hypersonic Speeds. AIAA-91-0199, Jan. 1991.
8. Chow, R.; and Marconi, F.: A Navier-Stokes Solution to Hypersonic Store Separation Flow Fields. AIAA-89-0031, Jan. 1989.
9. Keyes, J. W.: *Force Testing Manual for the Langley 20-Inch Mach 6 Tunnel*. NASA TM-74026, 1977.

Table I. Strain Gage Balance Accuracy

Balance component	Full-scale output	$\pm 0.5$ percent of full-scale output
Normal force, lb	15	$\pm 0.075$
Axial force, lb	3	$\pm 0.015$
Pitching moment, in-lb	10	$\pm 0.050$

Table II. Coefficient Uncertainties

Coefficient	Coefficient uncertainty for—	
	Cone cylinder	Roof delta
$C_N$	$\pm 0.059$	$\pm 0.0046$
$C_A$	$\pm 0.012$	$\pm 0.00092$
$C_m$	$\pm 0.040$	$\pm 0.00089$

Table III. Experimental Data

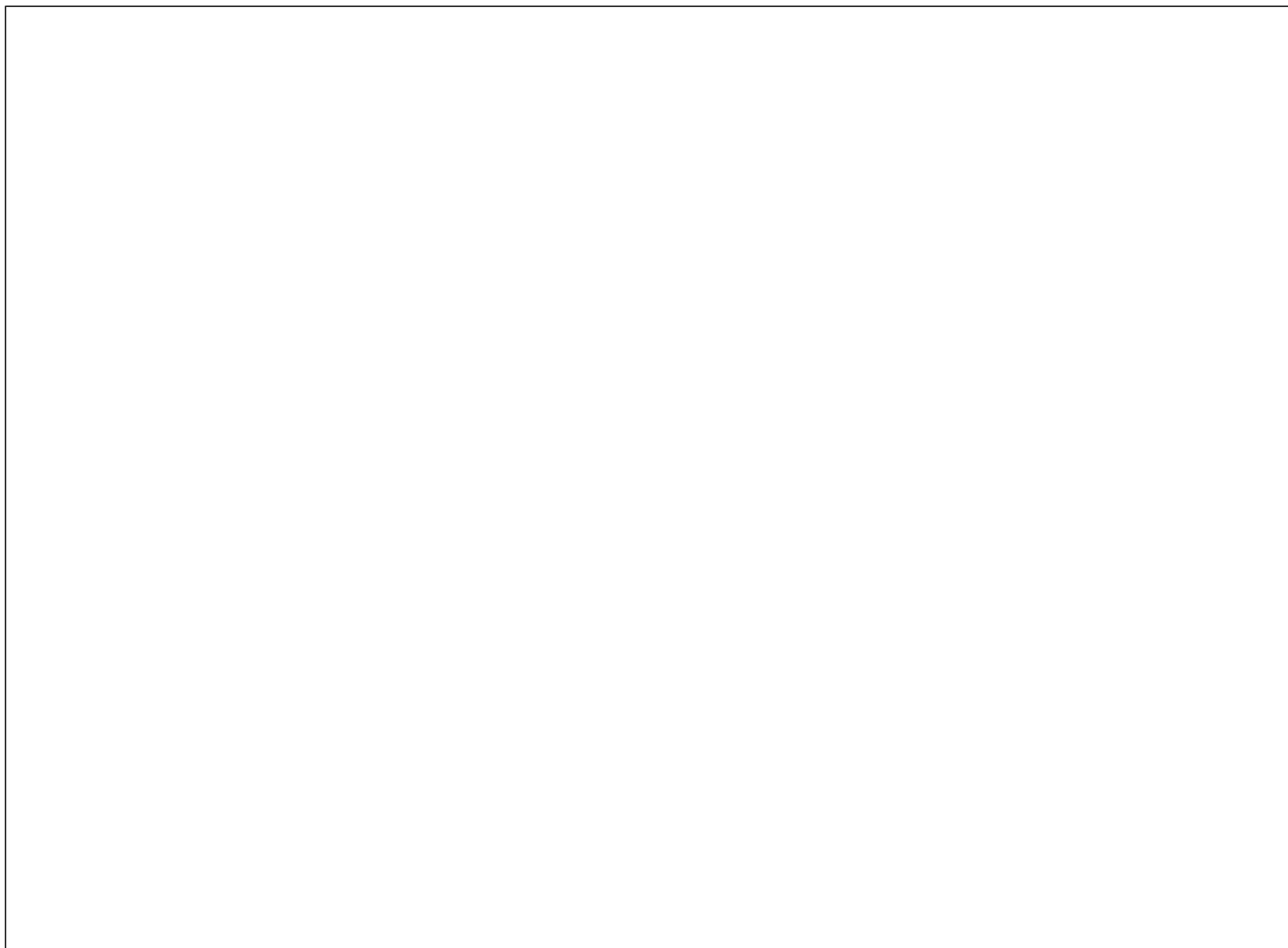
(a) Cone cylinder

$h$ , in.	$C_N$	$C_A$	$C_m$
$\alpha = 0^\circ$			
0.39	−0.1002	0.0080	−0.0444
.89	−.1909	.0586	−.2778
1.39	−.1570	.0672	−.1525
1.89	−.1450	.0567	−.1948
2.39	−.1608	.0582	−.2238
2.89	−.2149	.0786	−.1963
3.39	−.2264	.1100	−.1782
3.89	−.2070	.1302	−.1518
4.39	−.1730	.1554	−.0969
4.89	−.1220	.1893	−.0221
5.39	−.0191	.2223	.1296
5.89	.0307	.2170	.1019
6.39	.0461	.2141	.0162
6.89	.0464	.2109	.0244
7.39	.0480	.2125	.0368
$\alpha = 15^\circ$			
0.92	0.0023	0.0001	−0.0586
1.42	.0356	.0530	.0712
1.92	.1035	.0602	.1777
2.42	.1017	.0510	.0459
2.92	.1088	.0638	.0689
3.42	.1282	.0823	.1800
3.92	.1945	.1127	.3237
4.42	.2954	.1483	.4787
4.92	.4537	.1968	.6752
5.42	.6435	.2475	.9209
5.92	.8565	.2881	1.0834
6.42	.9898	.2819	.9959
6.92	1.0896	.2788	.8136
7.42	1.1669	.2810	.6301
7.92	1.2100	.2801	.5056
8.92	1.2000	.2813	.5537

(b) Roof delta

$h$ , in.	$C_N$	$C_A$	$C_m$
$\alpha = 0^\circ$			
0.40	−0.0525	0.0118	0.0004
.90	−.0596	.0132	−.0012
1.40	−.0642	.0149	.0002
1.90	−.0651	.0158	.0007
2.40	−.0735	.0181	.0009
2.90	−.0850	.0214	.0013
3.40	−.0911	.0233	.0008
3.90	−.0958	.0256	.0007
4.40	−.0978	.0276	.0008
4.90	−.0965	.0300	.0014
5.40	−.0878	.0323	.0032
5.90	−.0782	.0320	.0006
6.40	−.0784	.0314	−.0008
6.90	−.0800	.0318	.0006
7.40	−.0827	.0326	.0023
$\alpha = 15^\circ$			
0.40	−0.0022	−0.0038	0.0006
.90	−.0103	−.0007	−.0013
1.40	−.0075	.0007	.0012
1.90	.0032	.0014	.0003
2.40	.0035	.0008	−.0018
2.90	−.0002	.0006	−.0011
3.40	−.0009	.0016	.0029
3.90	.0083	.0030	.0052
4.40	.0223	.0056	.0093
4.90	.0443	.0066	.0144
5.40	.0744	.0077	.0216
5.90	.1119	.0086	.0254
6.40	.1501	.0094	.0209
6.90	.1803	.0097	.0100
7.40	.1993	.0102	−.0003
7.90	.1954	.0095	.0008
8.40	.1933	.0096	.0029

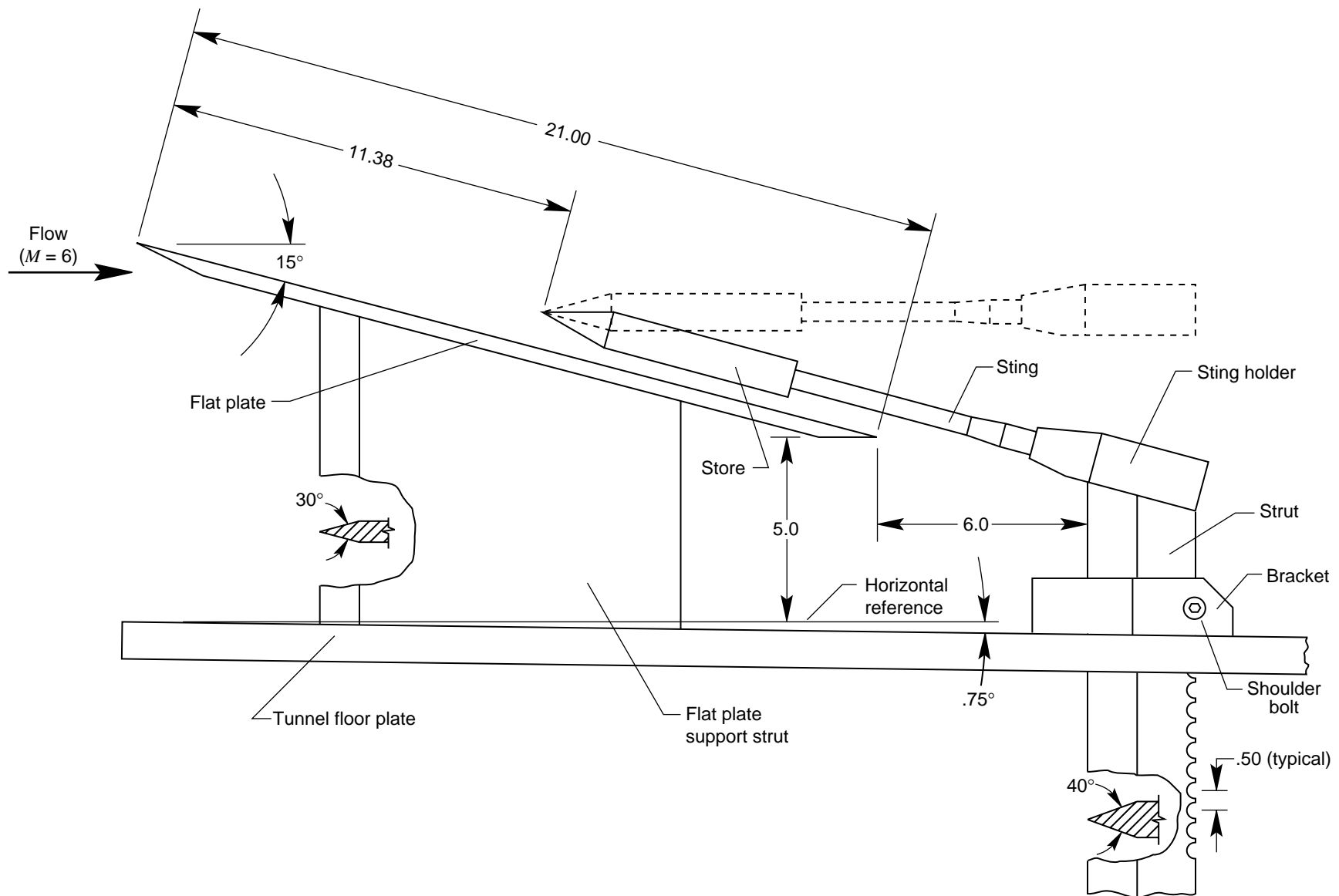




L-93-5561

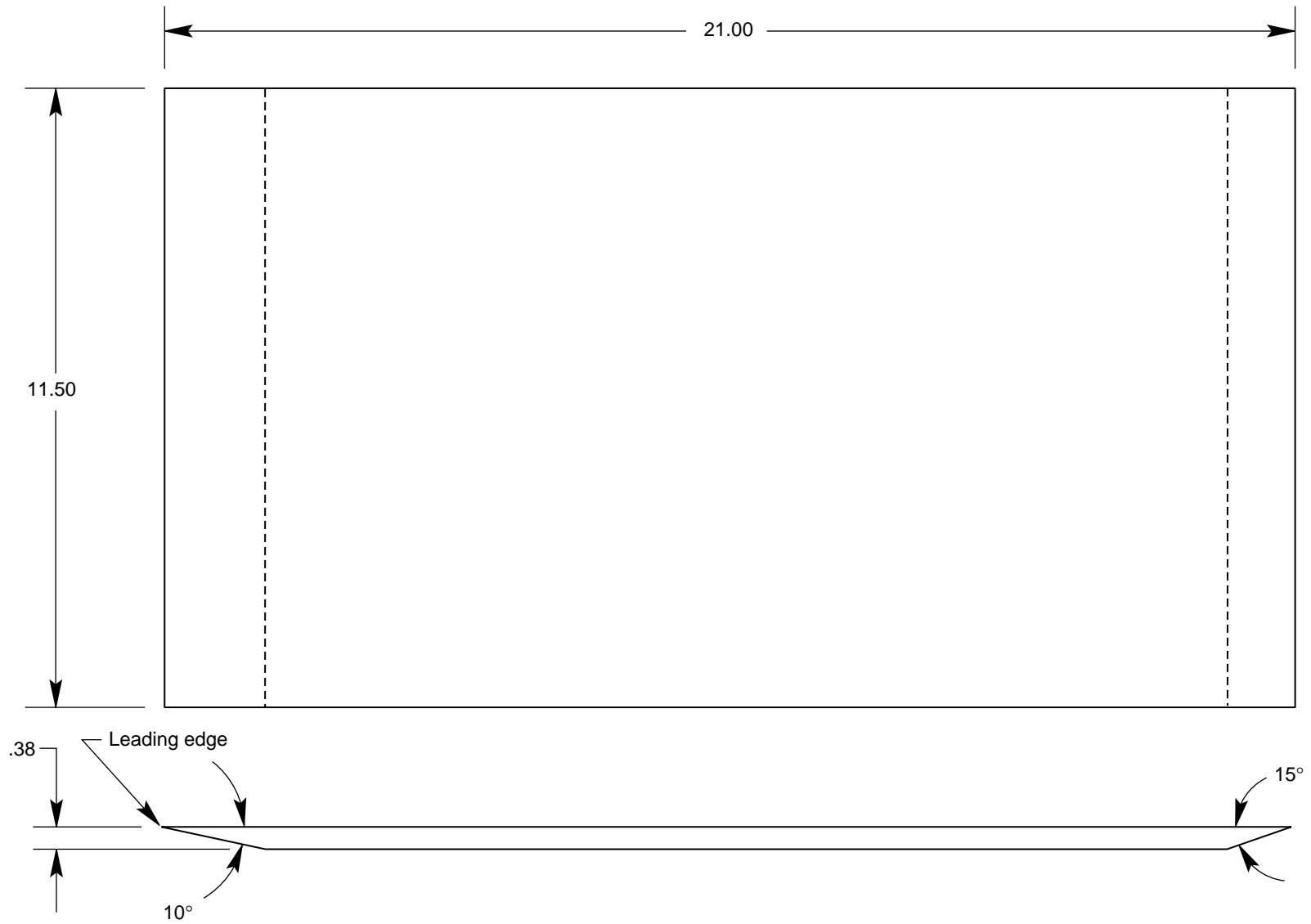
(a) Photograph of flat plate and store model mounted in wind tunnel.

Figure 1. Model test installation.



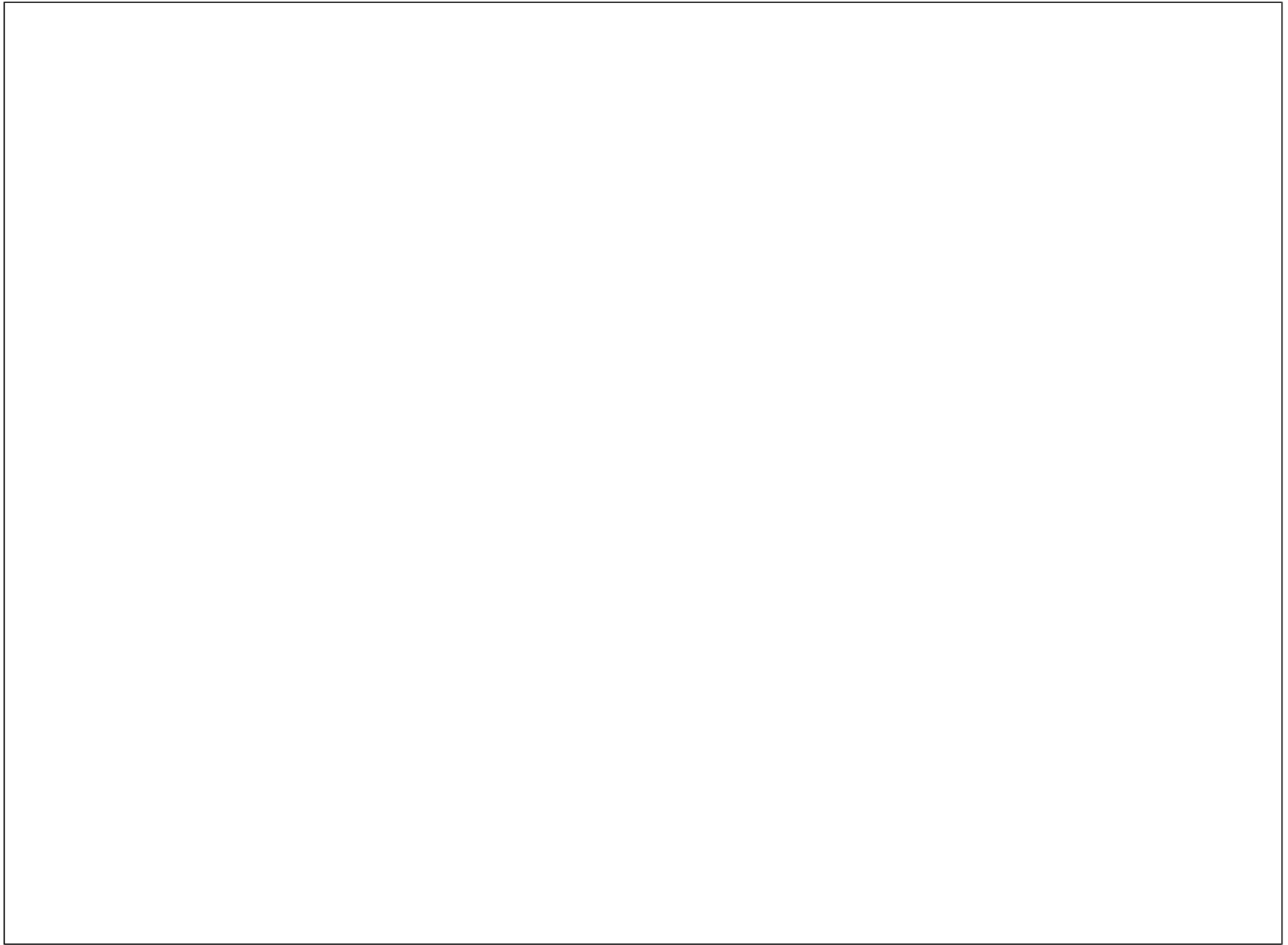
(b) Sketch of flat plate, store model, and support struts. All linear dimensions are in inches.

Figure 1. Continued.



(c) Sketch of flat plate. All linear dimensions are in inches.

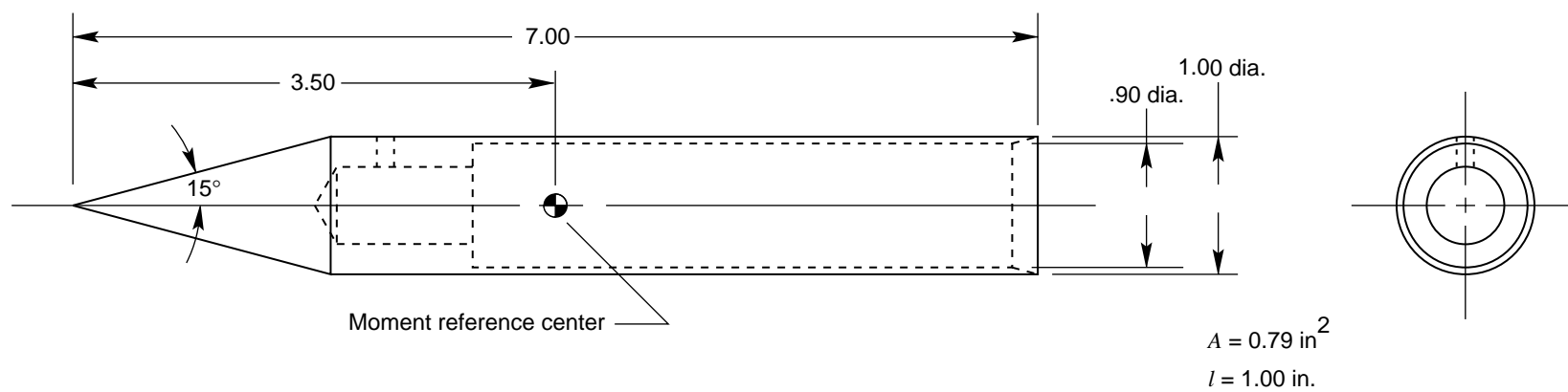
Figure 1. Concluded.



L-93-6142

(a) Photograph of store models.

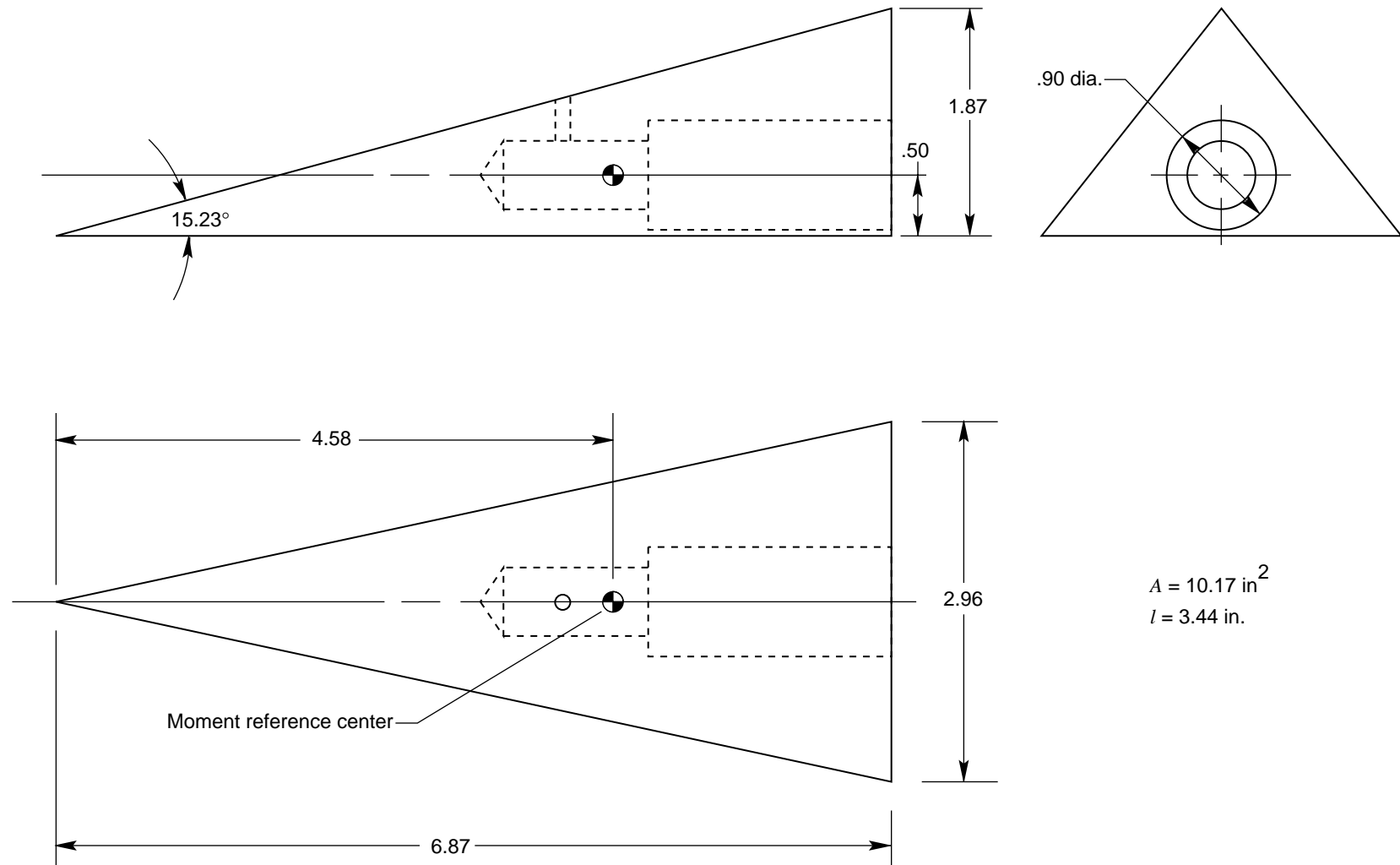
Figure 2. Description of store models.



(b) Cone cylinder model. All linear dimensions are in inches.

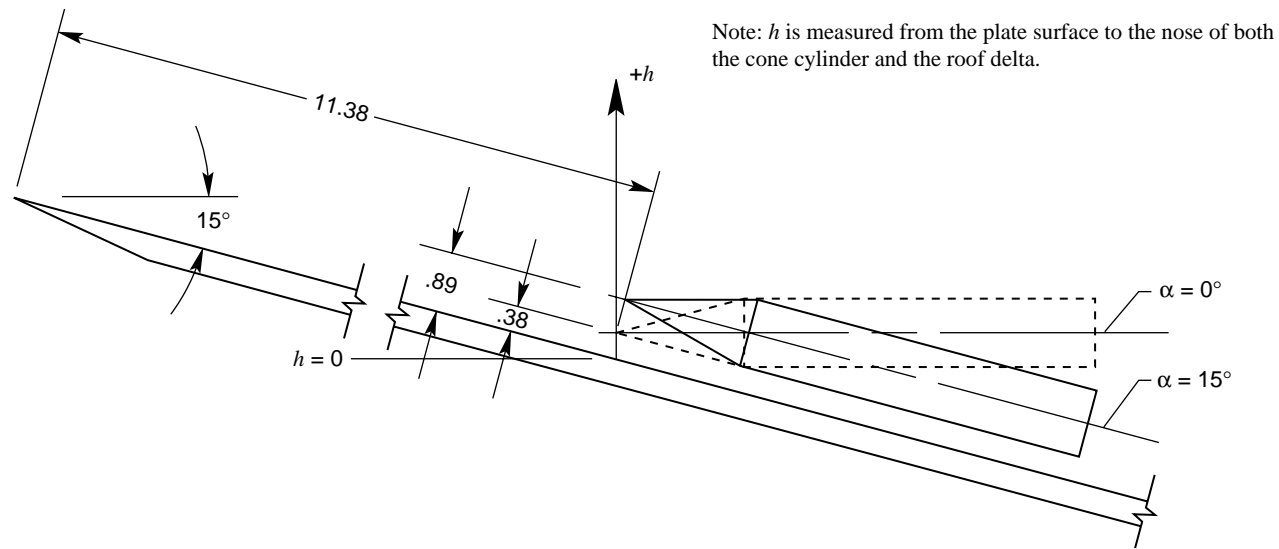
Figure 2. Continued.



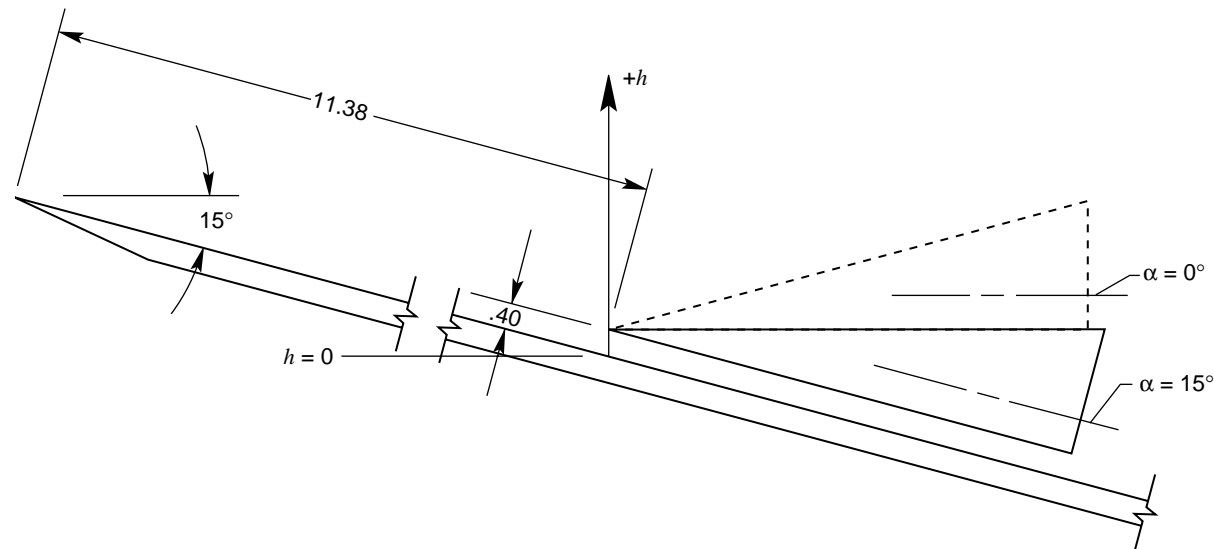


(c) Roof delta model. All linear dimensions are in inches.

Figure 2. Concluded.



(a) Cone cylinder.



(b) Roof delta.

Figure 3. Location of stores relative to flat plate at lowest store separation heights. All linear dimensions are in inches.

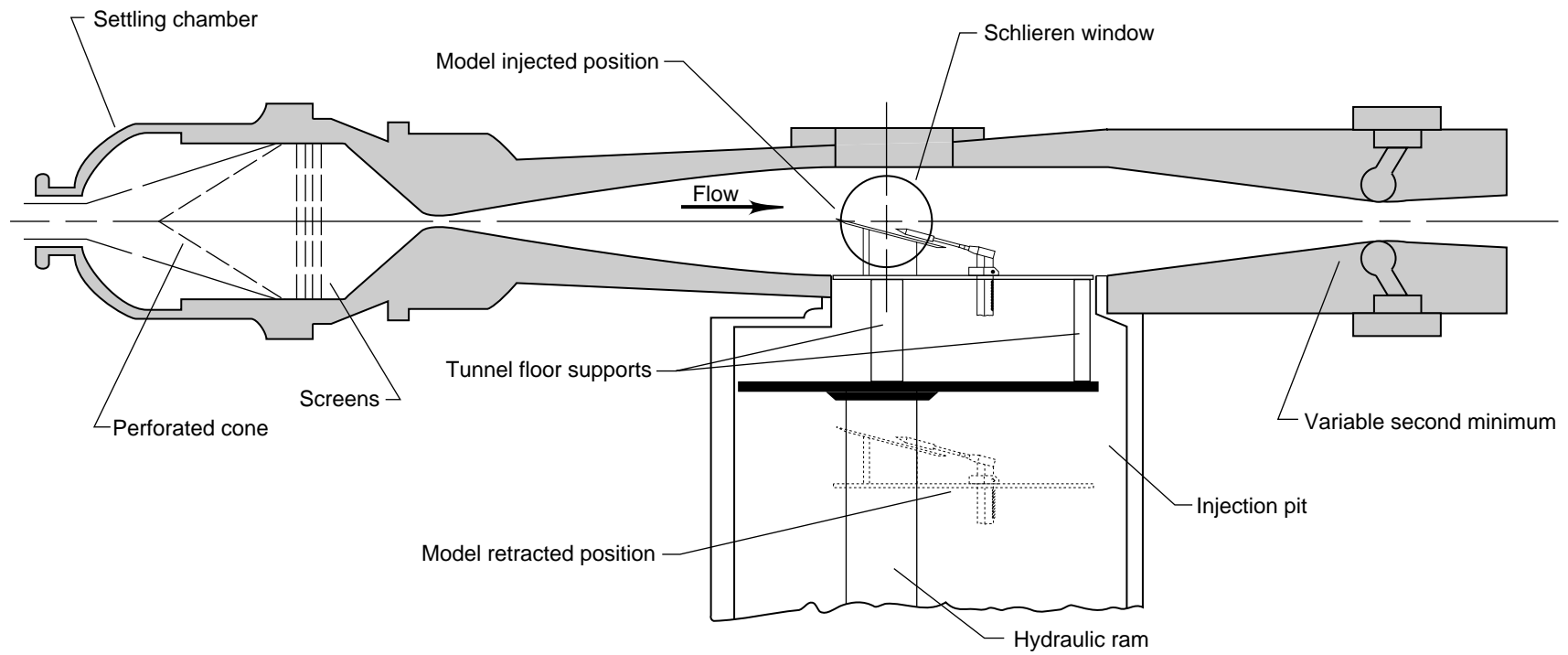
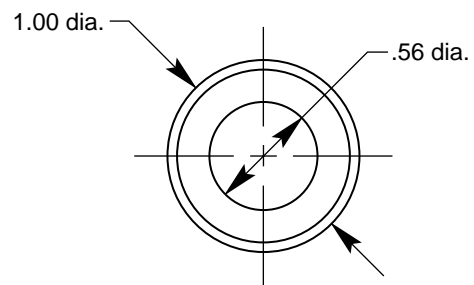
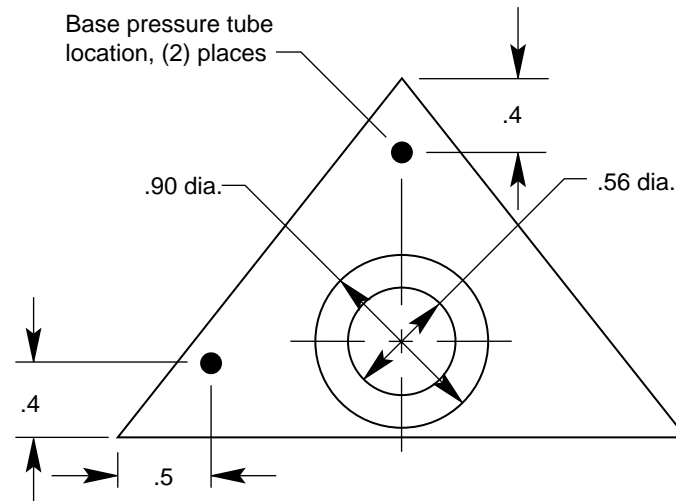


Figure 4. Langley 20-Inch Mach 6 Tunnel.



Base area = (not applicable)  
Chamber area =  $0.79 \text{ in}^2$

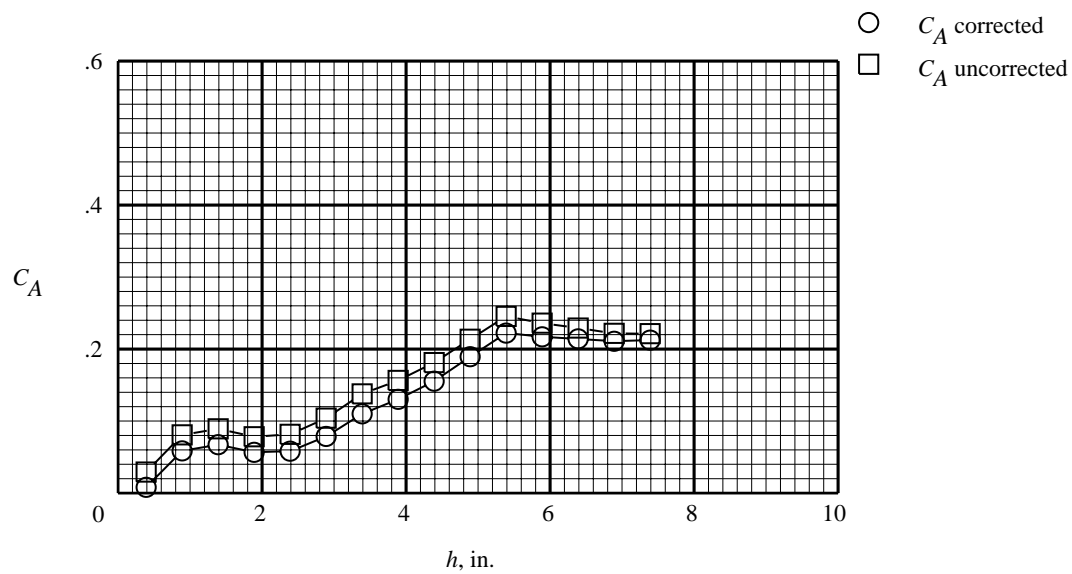
(a) Cone cylinder.



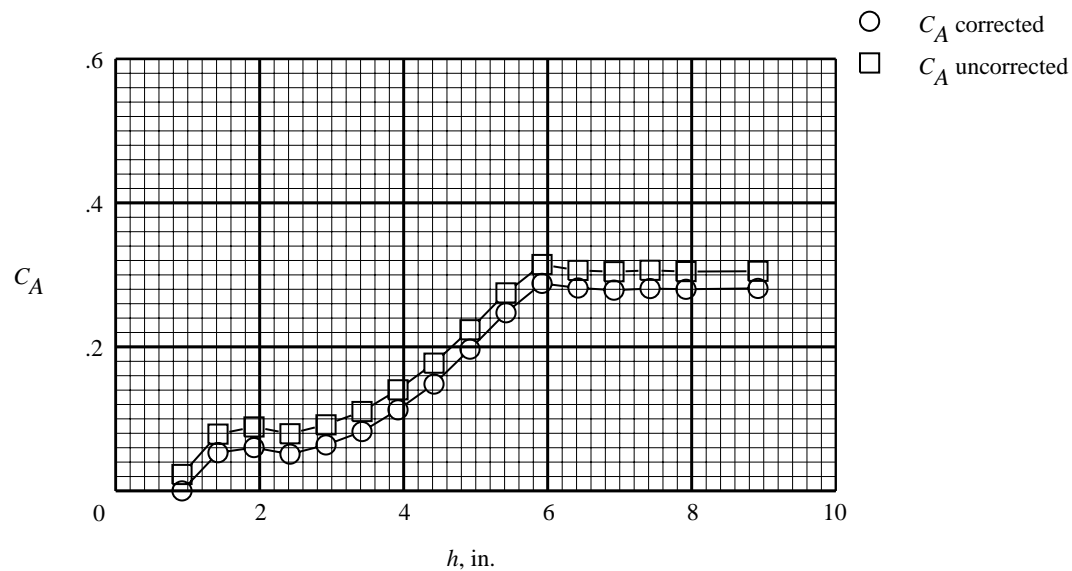
Base area =  $2.13 \text{ in}^2$   
Chamber area =  $0.64 \text{ in}^2$

(b) Roof delta.

Figure 5. Store model base and chamber areas. All linear dimensions are in inches.

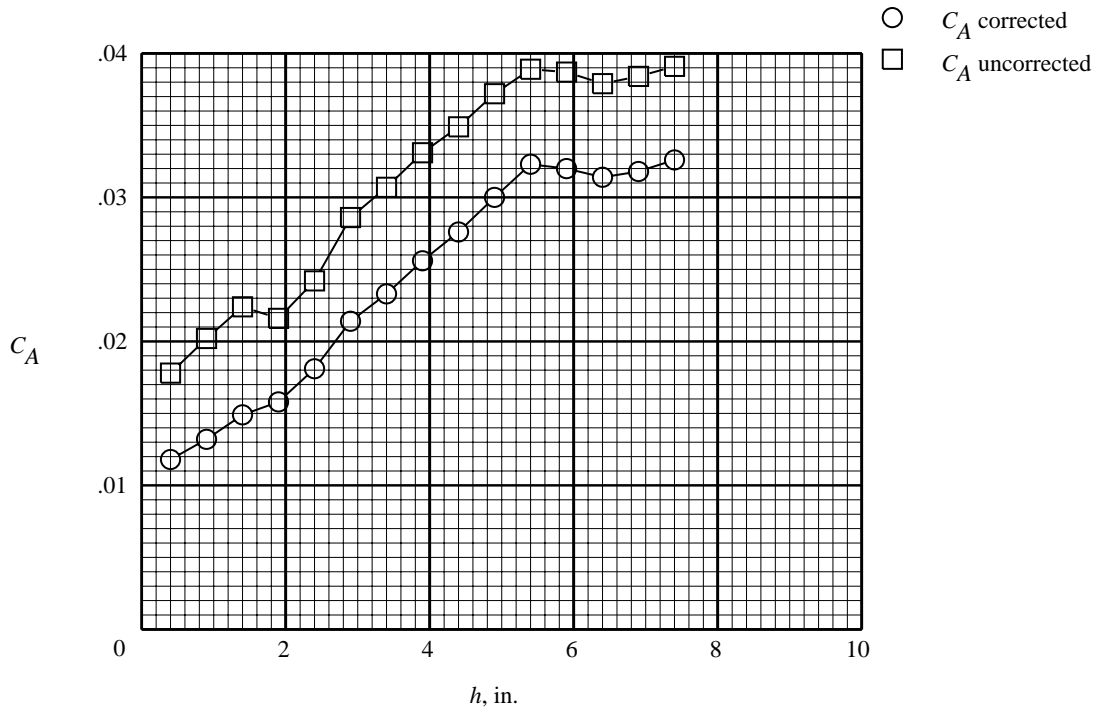


(a) Cone cylinder at  $\alpha = 0^\circ$ .

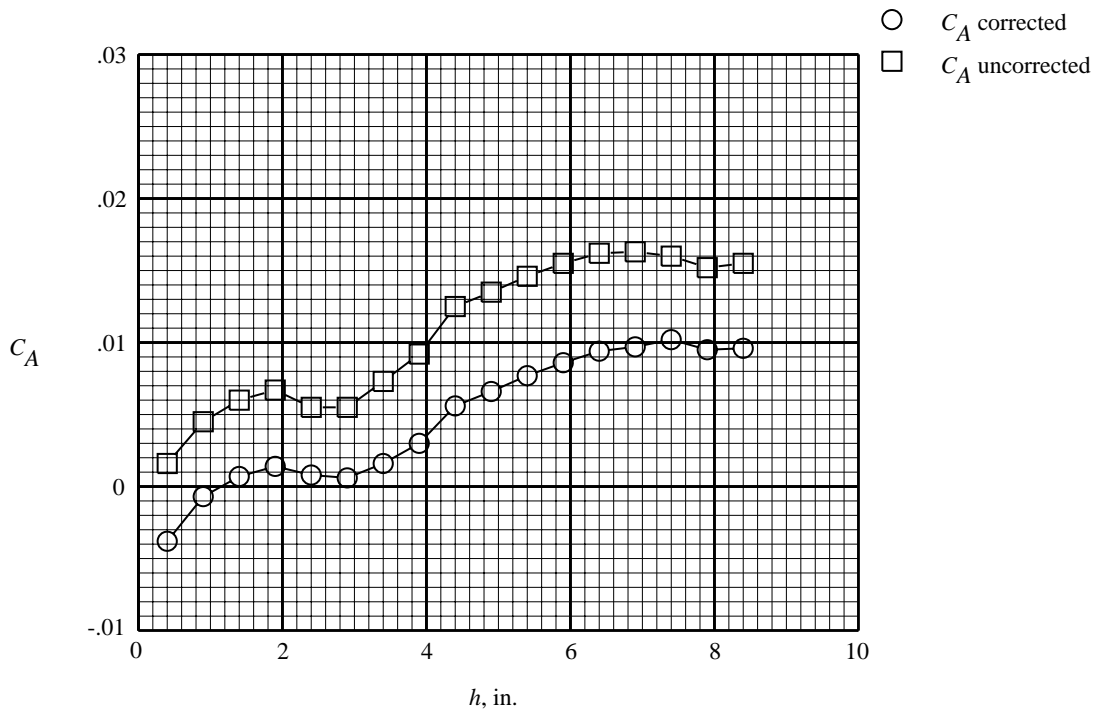


(b) Cone cylinder at  $\alpha = 15^\circ$ .

Figure 6. Corrected and uncorrected axial-force coefficients.



(c) Roof delta at  $\alpha = 0^\circ$ .



(d) Roof delta at  $\alpha = 15^\circ$ .

Figure 6. Concluded.

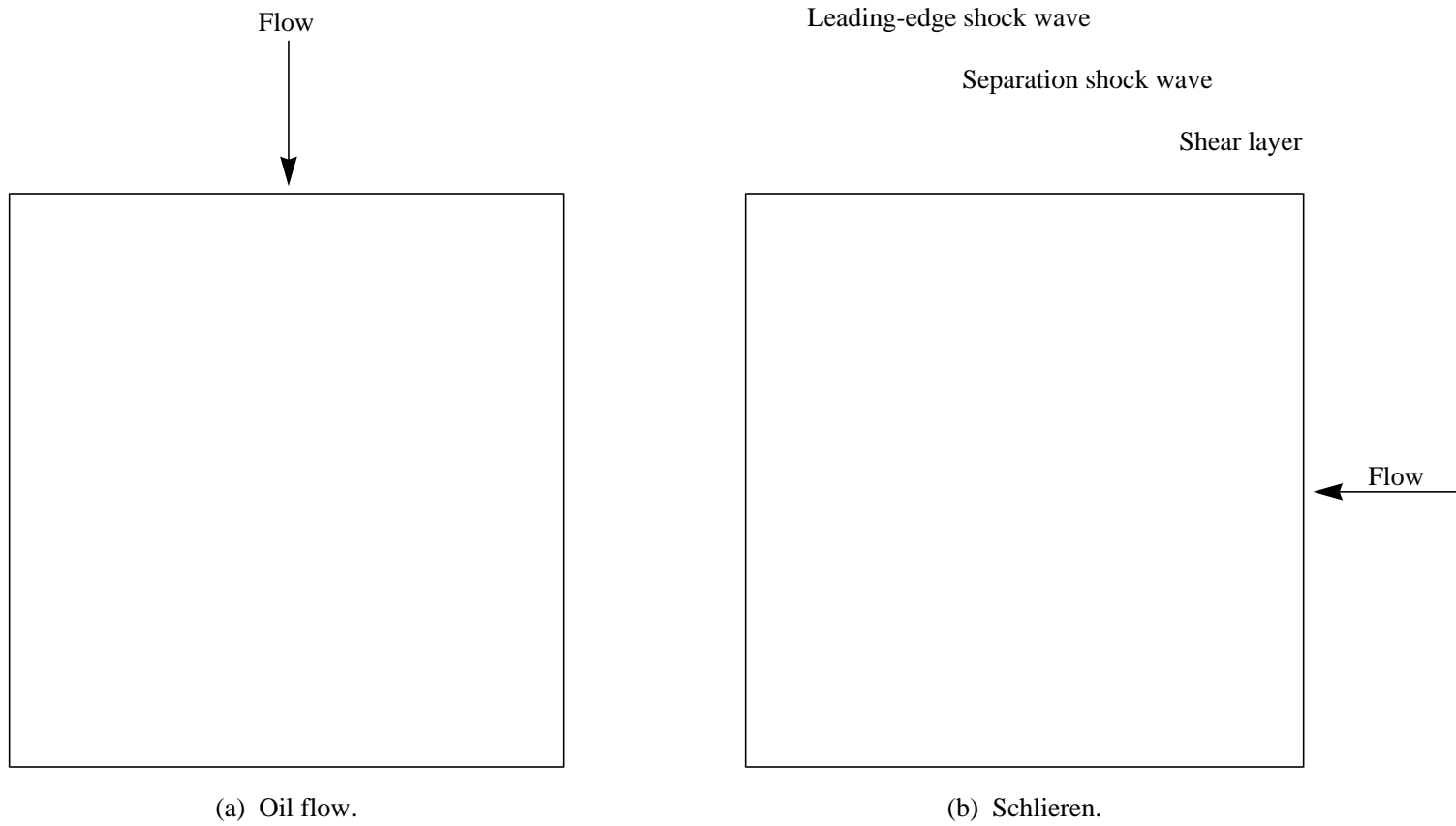


Figure 7. Flat plate flow visualization photographs.

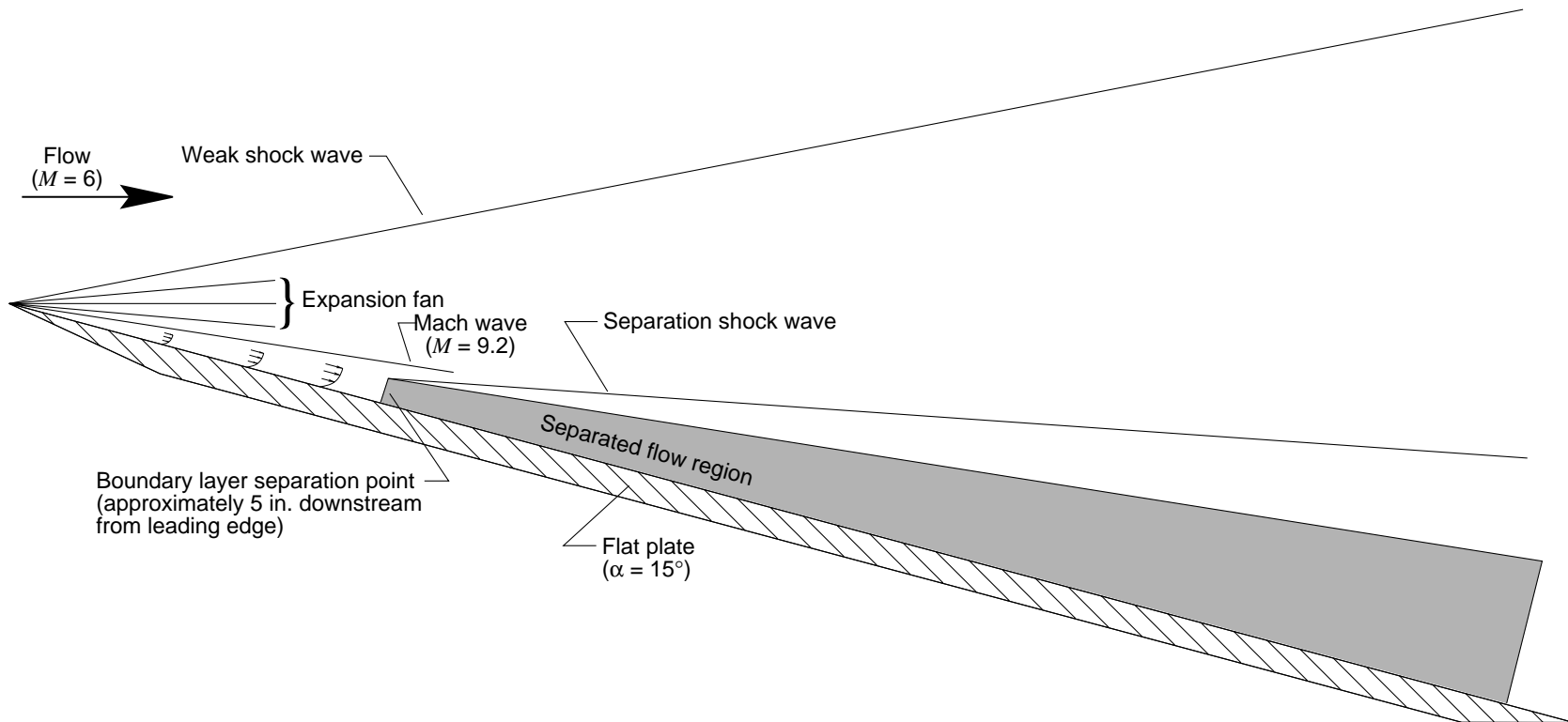
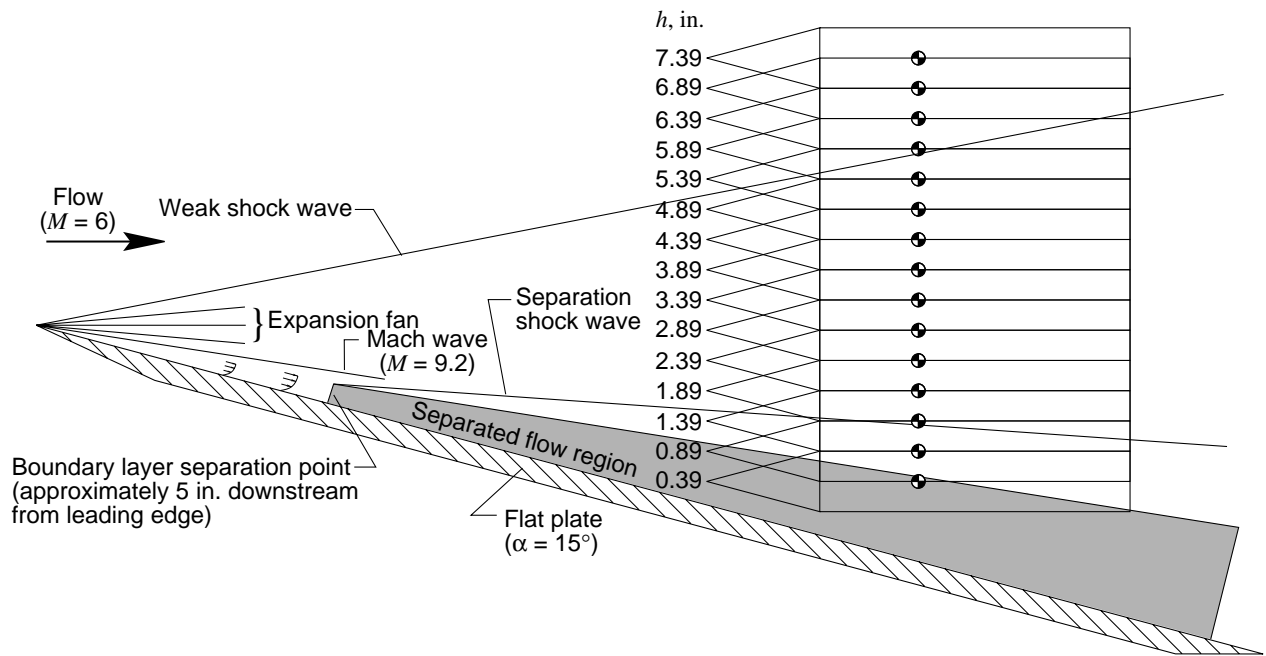
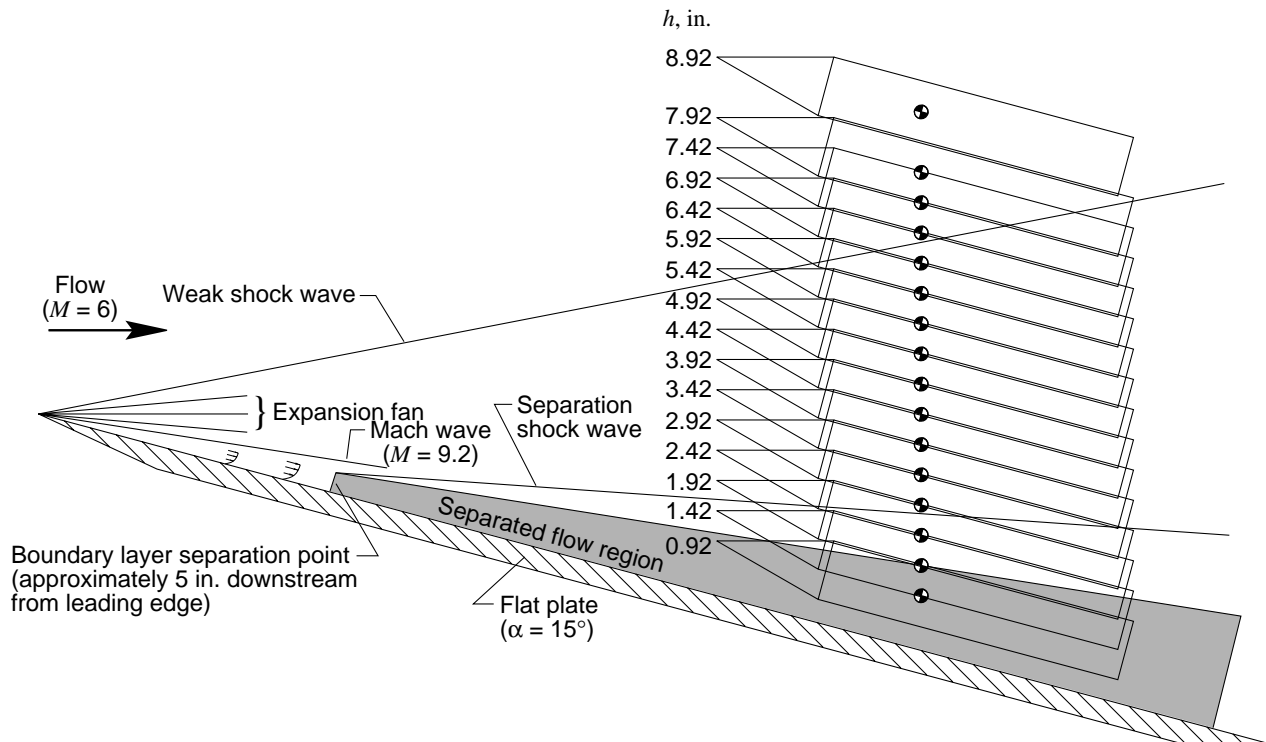


Figure 8. Sketch of flat plate flow field based on oil flow and schlieren photographs.





(a) Positions of cone cylinder at  $\alpha = 0^\circ$ .



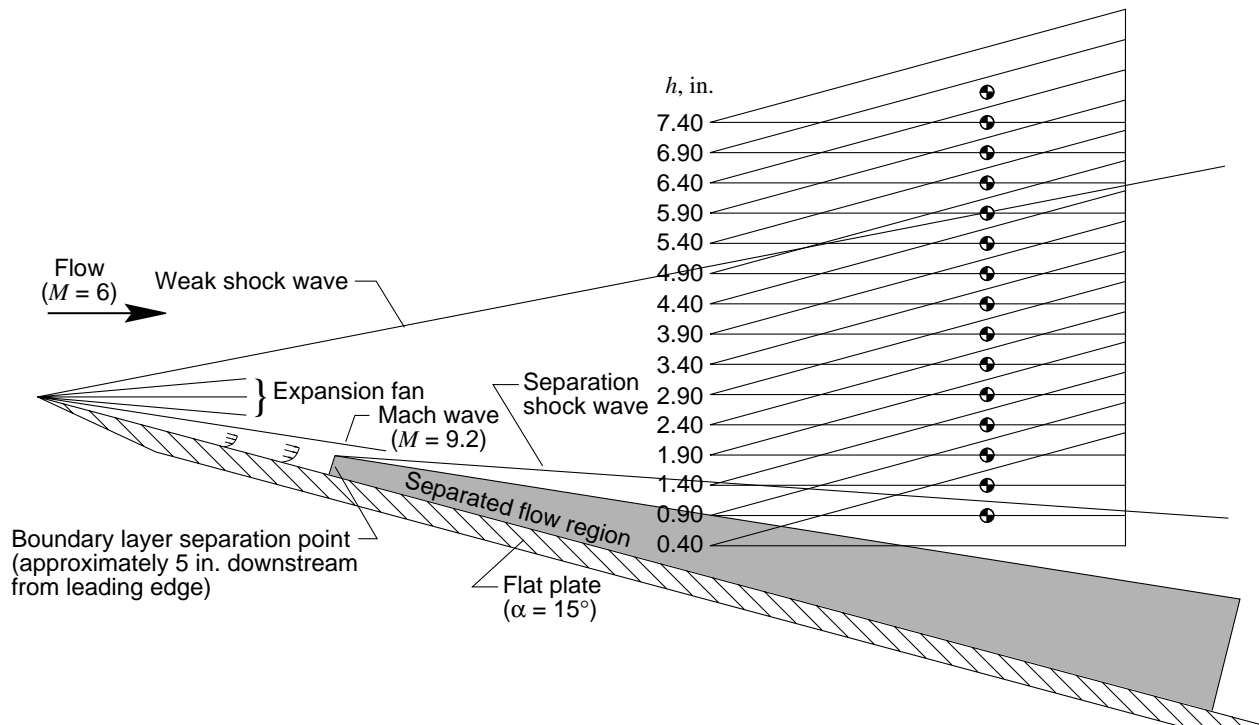
(b) Positions of cone cylinder at  $\alpha = 15^\circ$ .

Figure 9. Cone cylinder separation positions and characteristics in flat plate flow field.

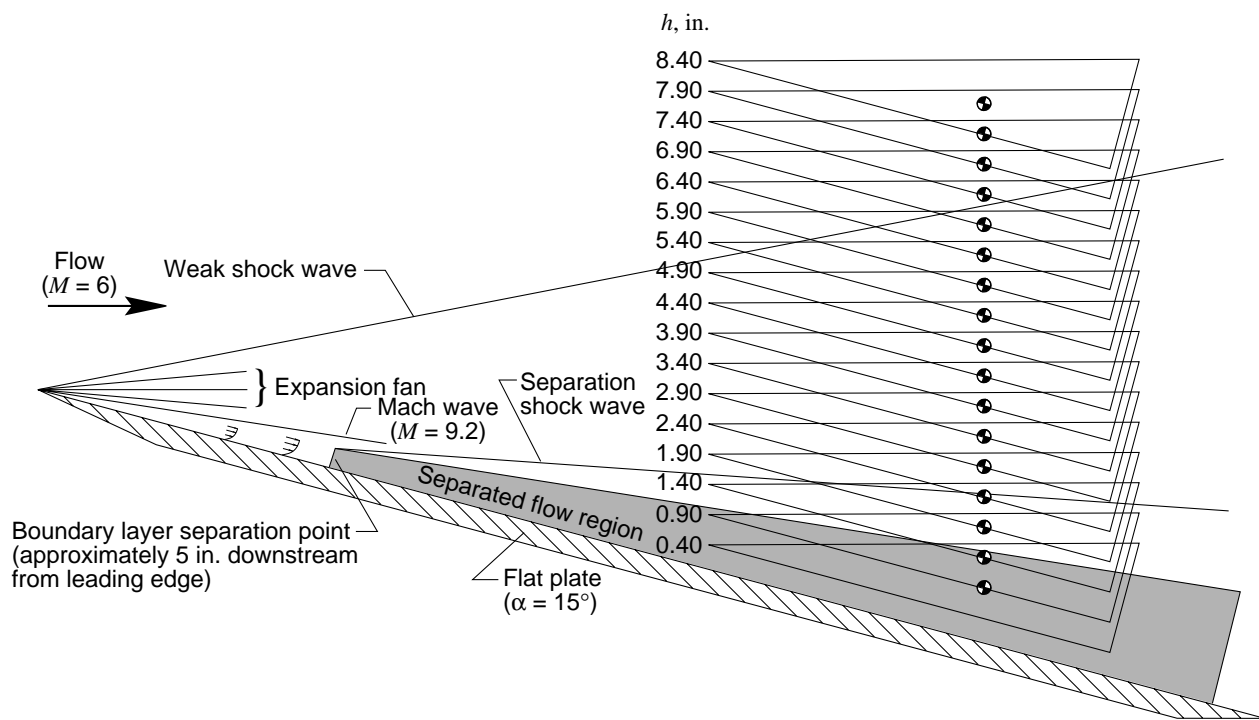


(c) Separation characteristics of cone cylinder.

Figure 9. Concluded.

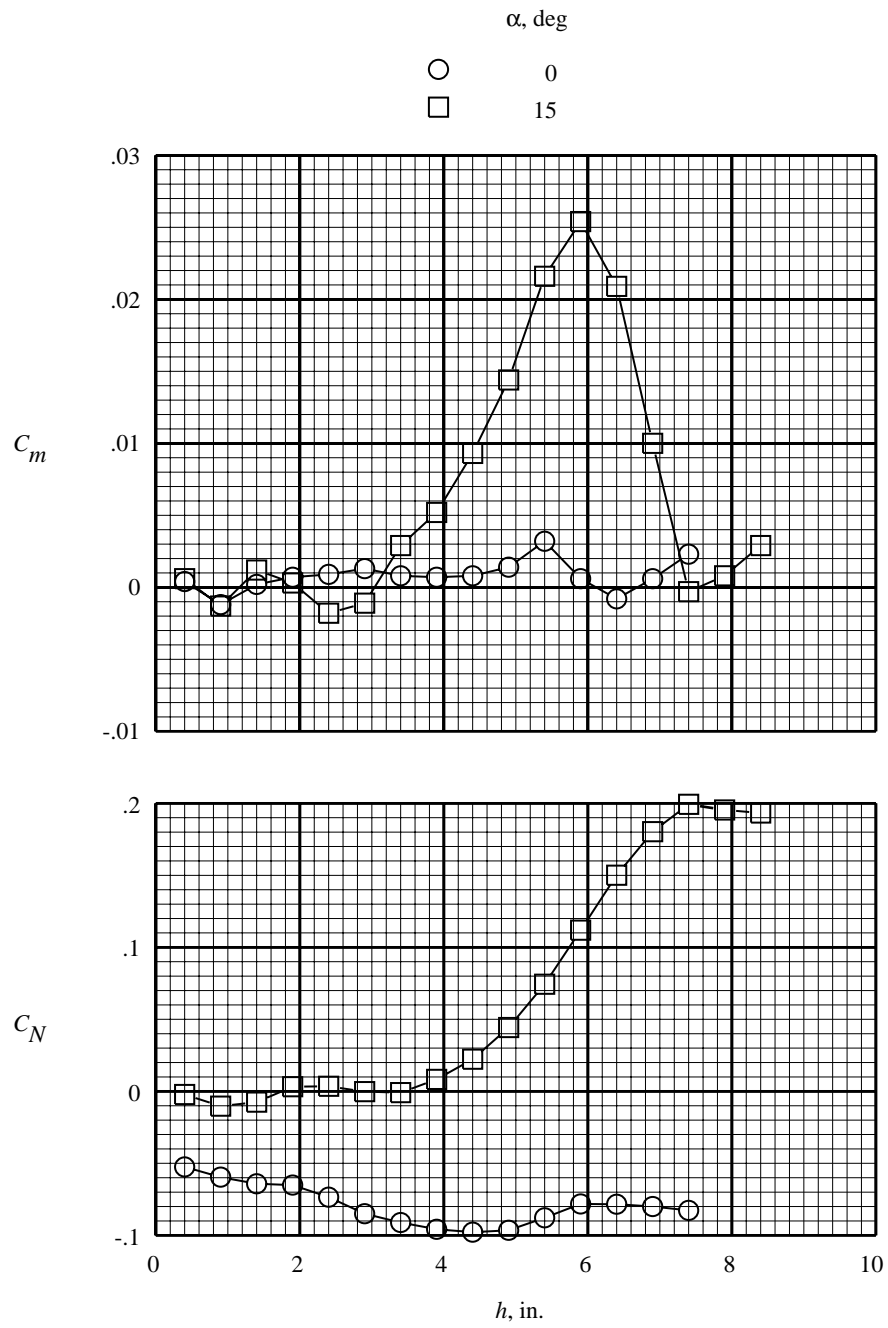


(a) Positions of roof delta at  $\alpha = 0^\circ$ .



(b) Positions of roof delta at  $\alpha = 15^\circ$ .

Figure 10. Roof delta separation positions and characteristics in flat plate flow field.



(c) Separation characteristics of roof delta.

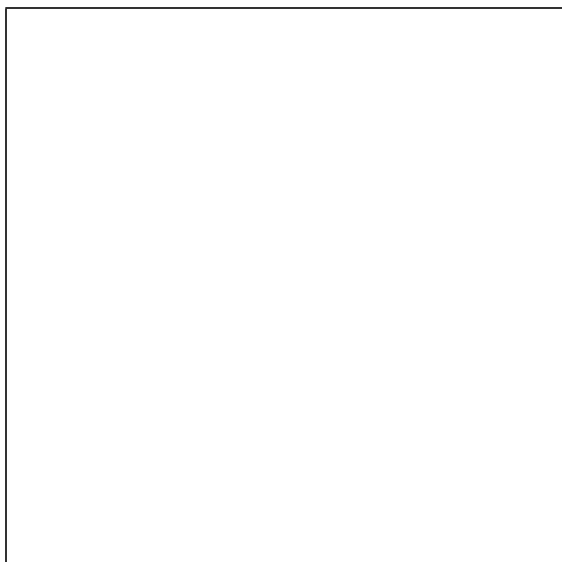
Figure 10. Concluded.

## Appendix

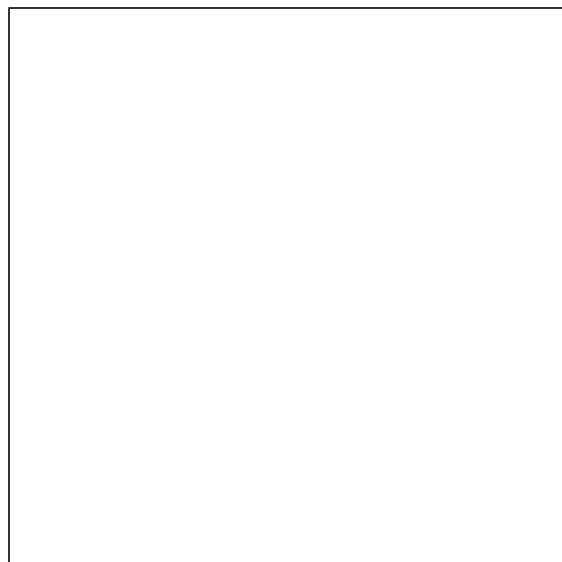
### Schlieren Photographs

Schlieren photographs of the cone cylinder and the roof delta at all store separation heights are presented in the following figures:

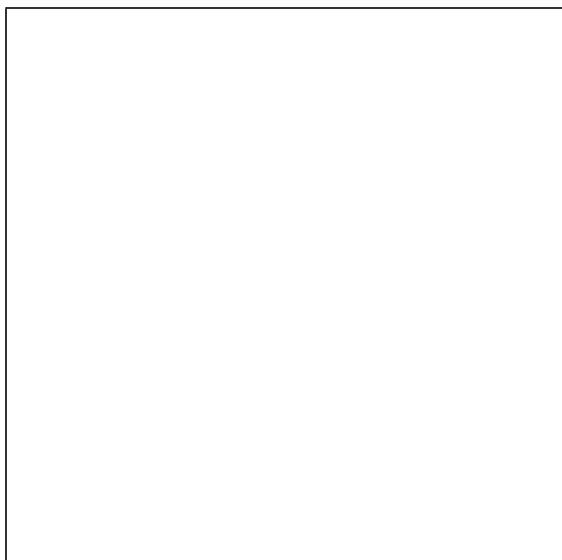
	Figure
Cone cylinder at $\alpha = 0^\circ$ .....	A1
Cone cylinder at $\alpha = 15^\circ$ .....	A2
Roof delta at $\alpha = 0^\circ$ .....	A3
Roof delta at $\alpha = 15^\circ$ .....	A4



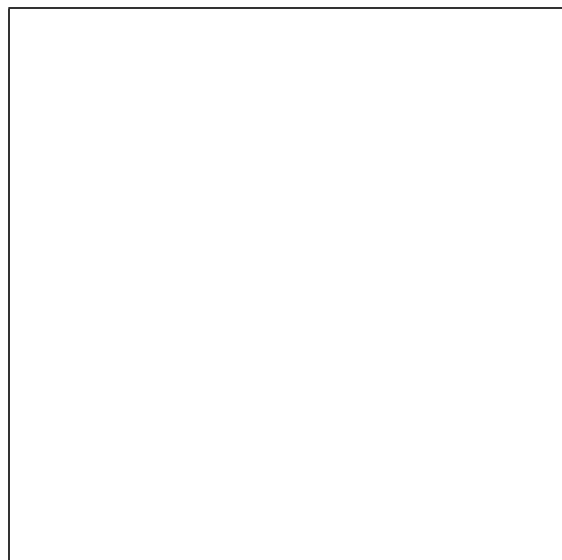
(a)  $h = 0.39$  in.



(b)  $h = 0.89$  in.

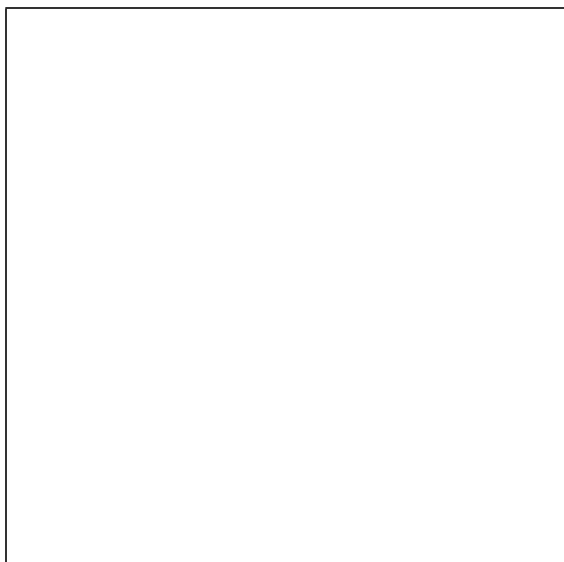


(c)  $h = 1.39$  in.

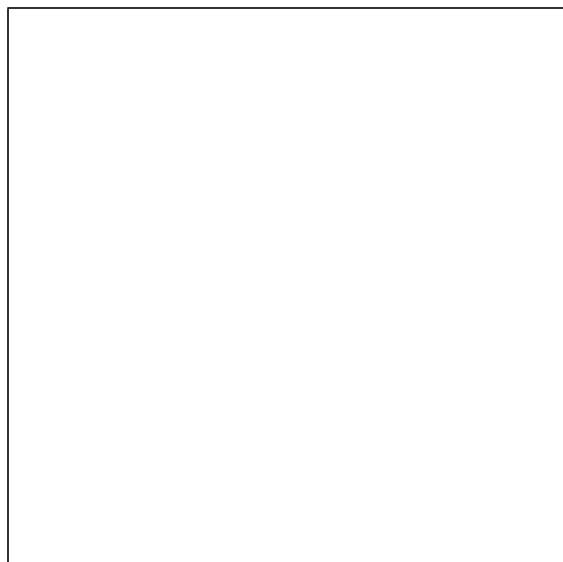


(d)  $h = 1.89$  in.

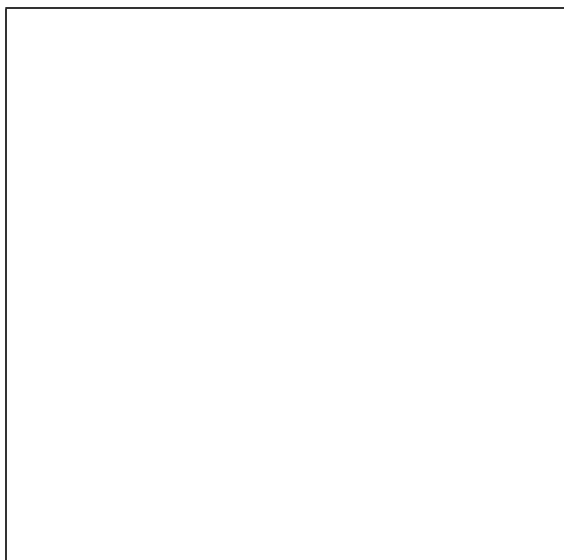
Figure A1. Schlieren photographs of cone cylinder at  $\alpha = 0^\circ$ . Flow is from right to left.



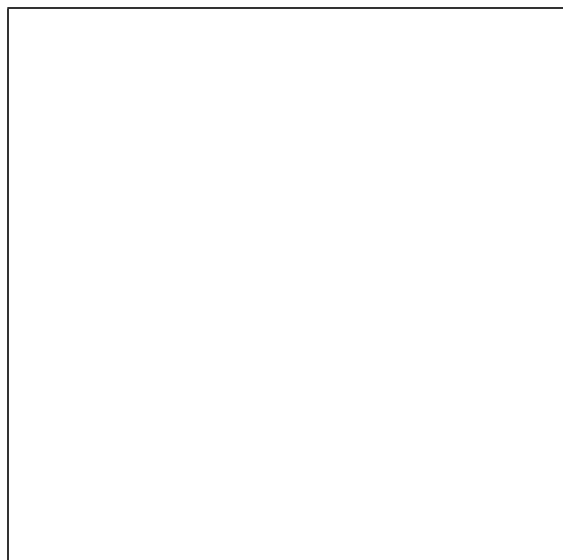
(e)  $h = 2.39$  in.



(f)  $h = 2.89$  in.

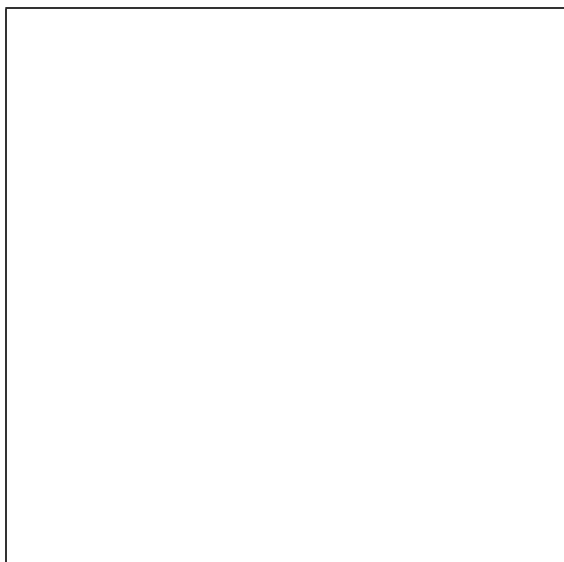


(g)  $h = 3.39$  in.

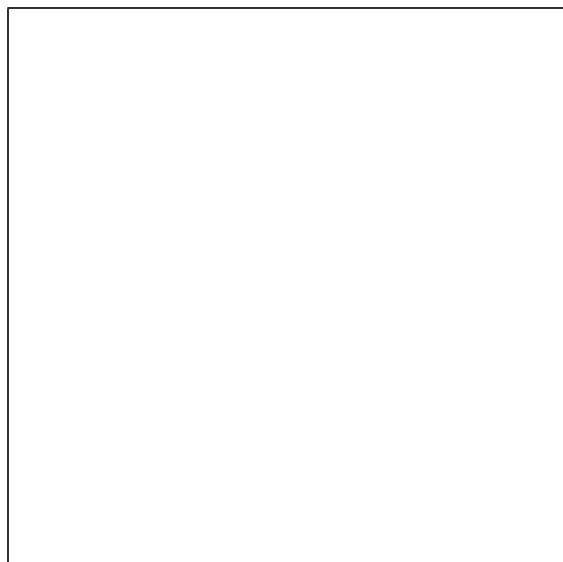


(h)  $h = 3.89$  in.

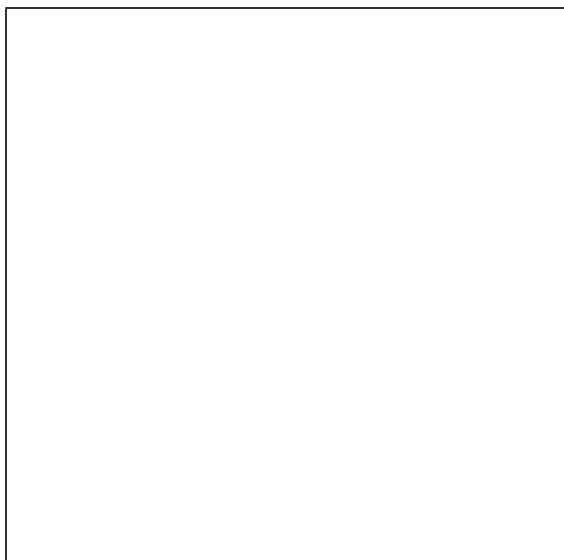
Figure A1. Continued.



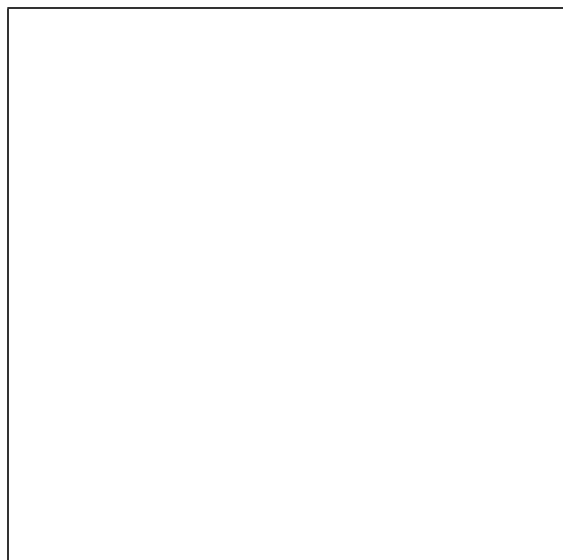
(i)  $h = 4.39$  in.



(j)  $h = 4.89$  in.



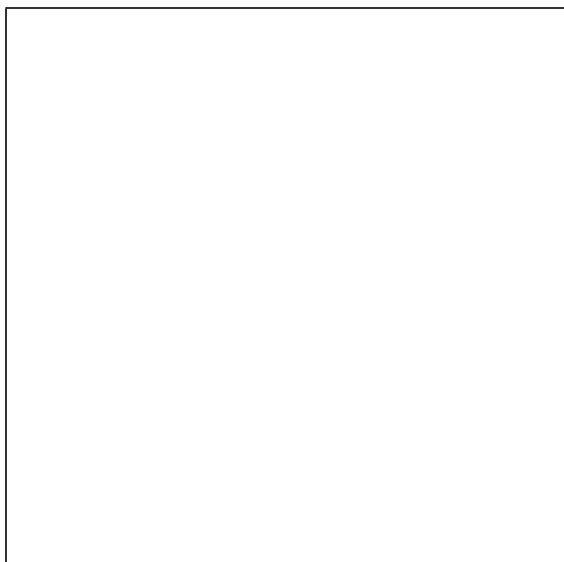
(k)  $h = 5.39$  in.



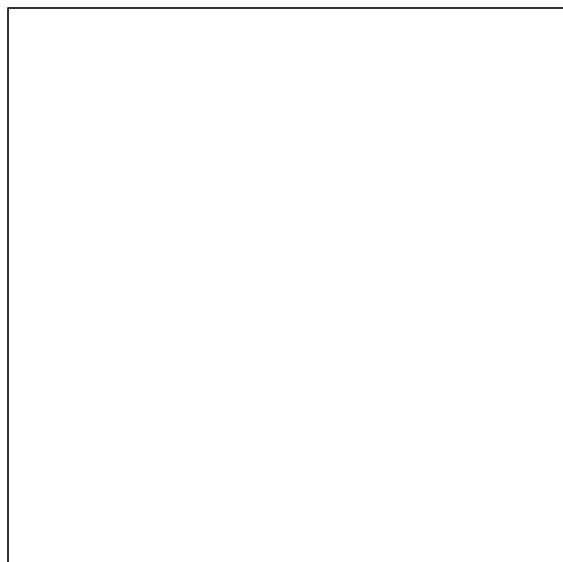
(l)  $h = 5.89$  in.

Figure A1. Continued.

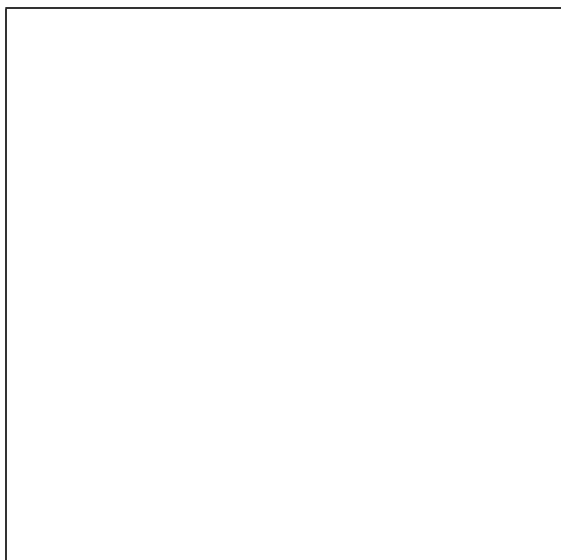




(m)  $h = 6.39$  in.

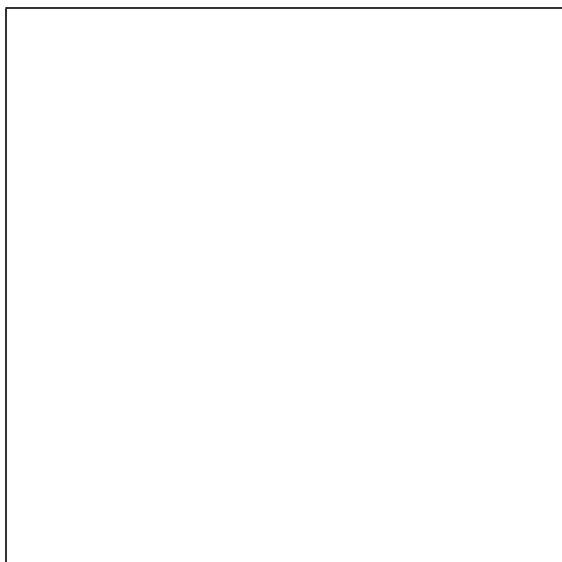


(n)  $h = 6.89$  in.

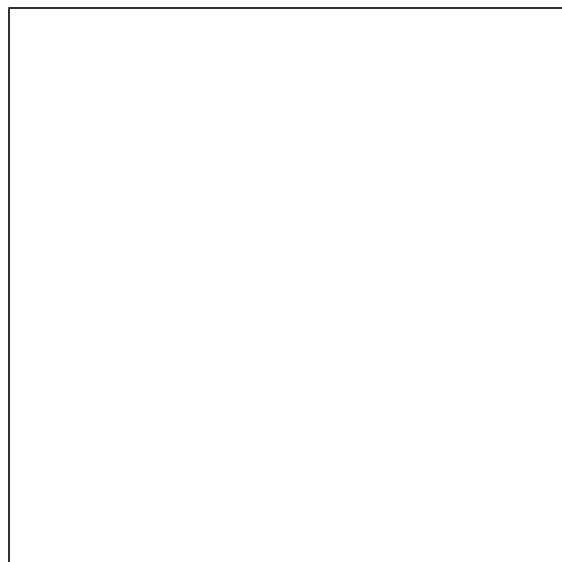


(o)  $h = 7.39$  in.

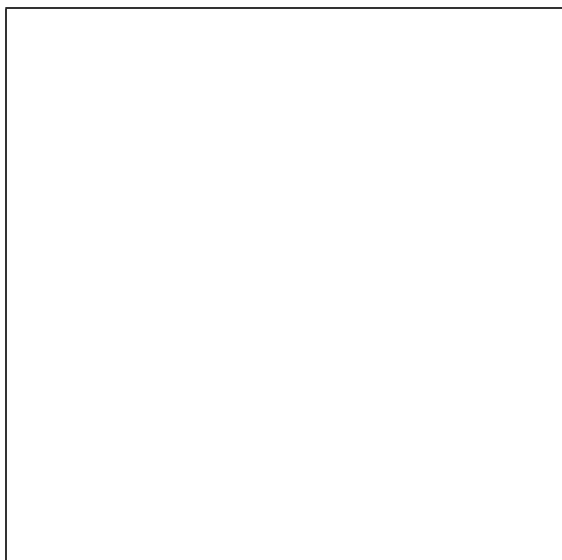
Figure A1. Concluded.



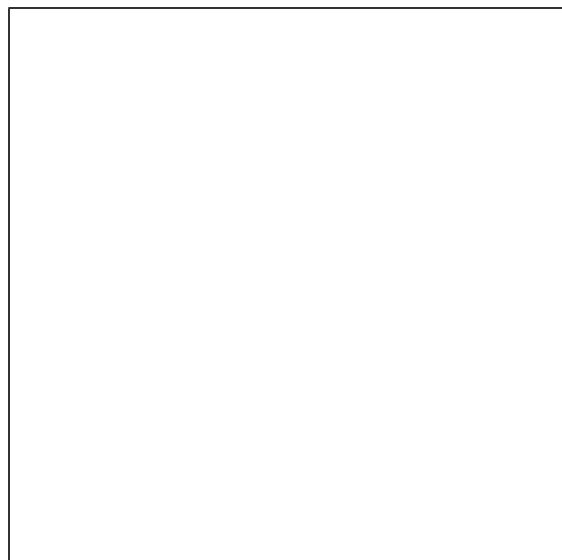
(a)  $h = 0.92$  in.



(b)  $h = 1.42$  in.

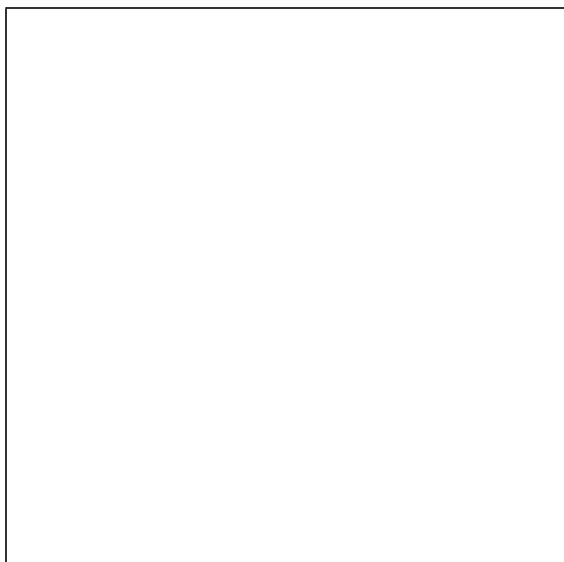


(c)  $h = 1.92$  in.

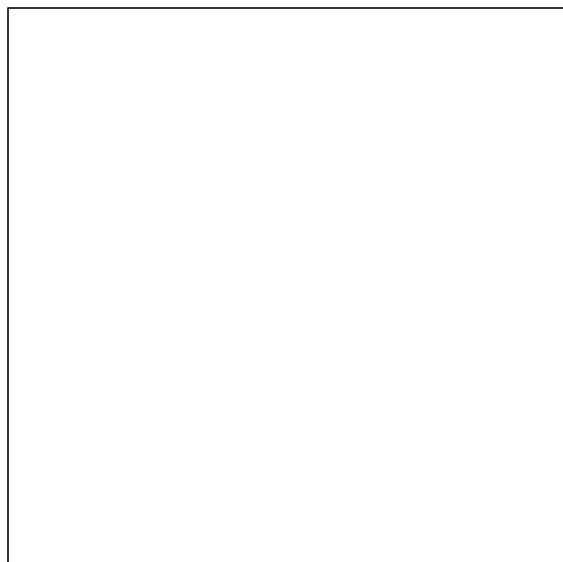


(d)  $h = 2.42$  in.

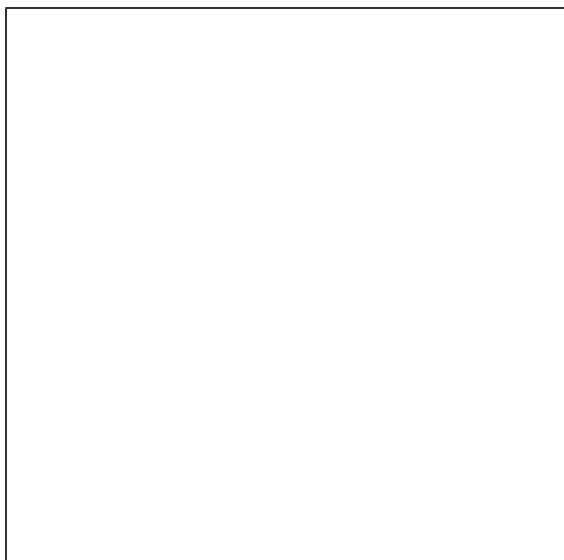
Figure A2. Schlieren photographs of cone cylinder at  $\alpha = 15^\circ$ . Flow is from right to left.



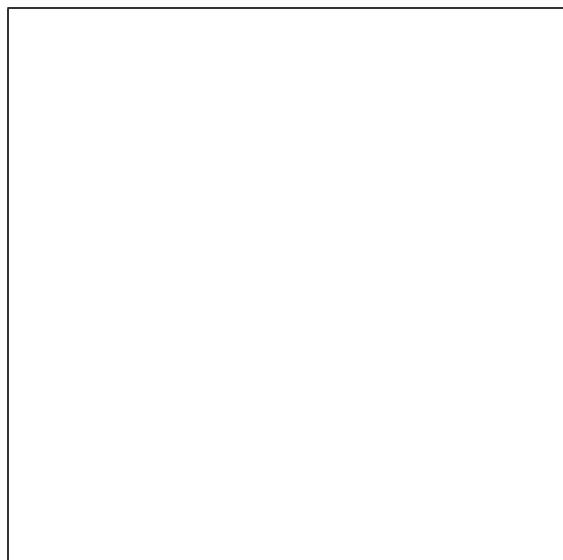
(e)  $h = 2.92$  in.



(f)  $h = 3.42$  in.

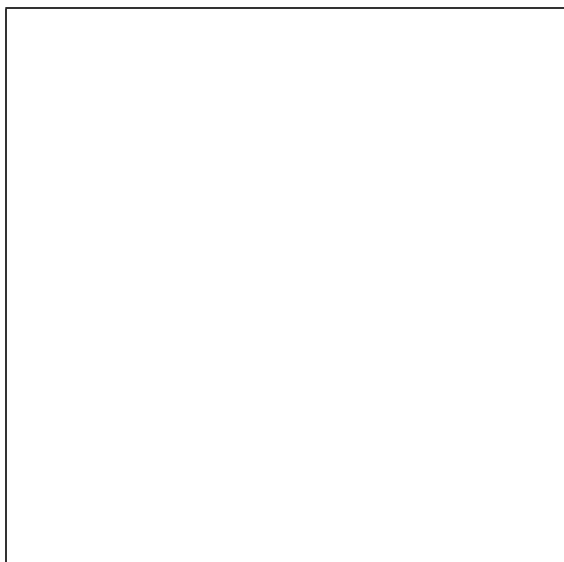


(g)  $h = 3.92$  in.

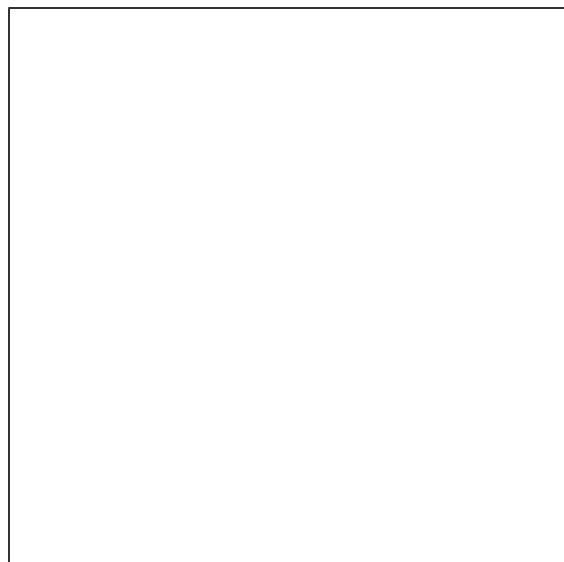


(h)  $h = 4.42$  in.

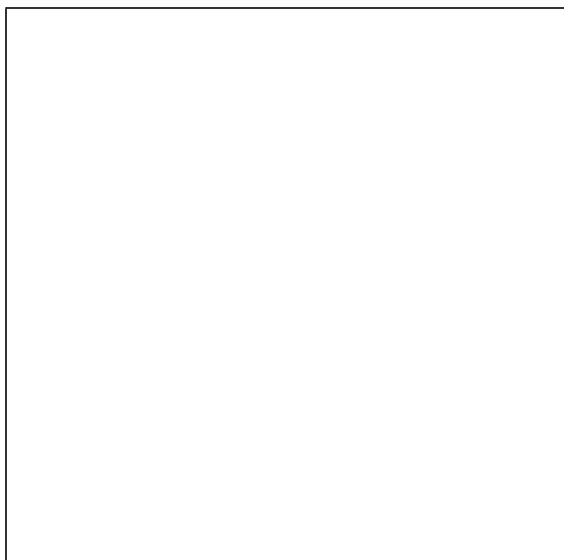
Figure A2. Continued.



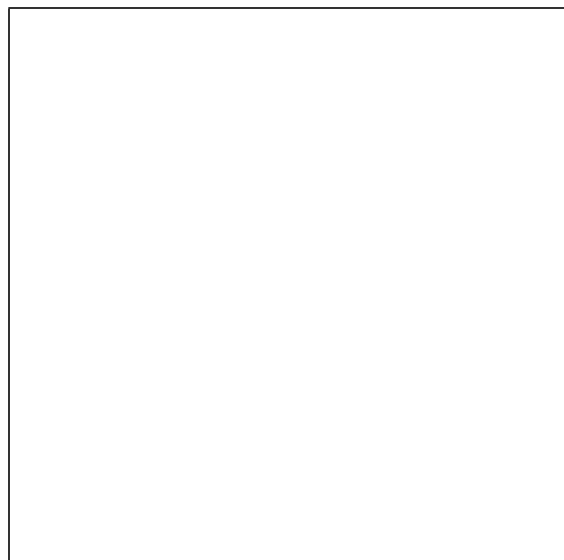
(i)  $h = 4.92$  in.



(j)  $h = 5.42$  in.

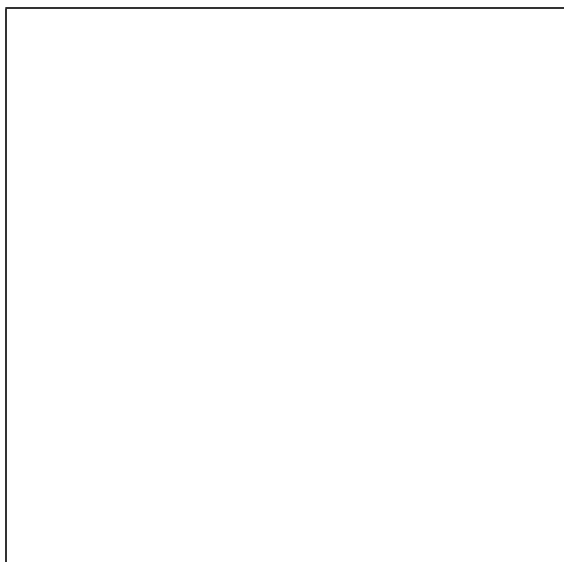


(k)  $h = 5.92$  in.

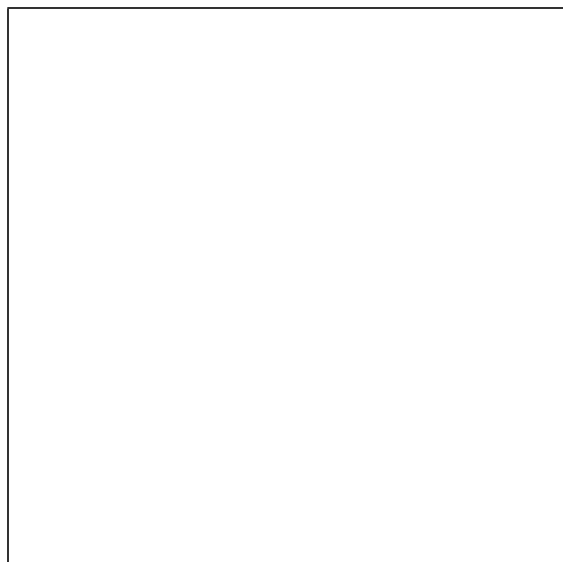


(l)  $h = 6.42$  in.

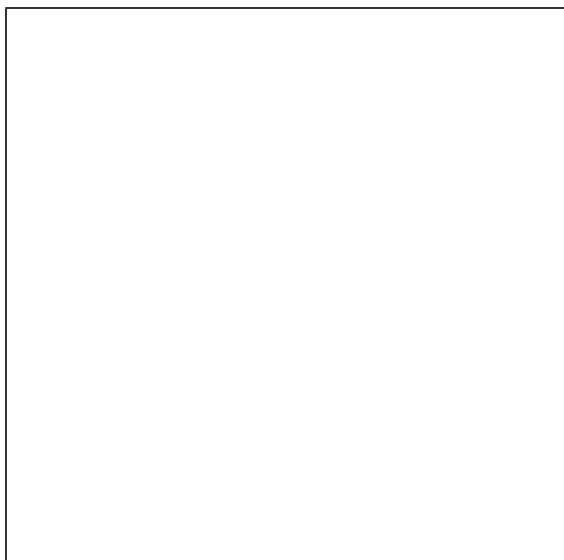
Figure A2. Continued.



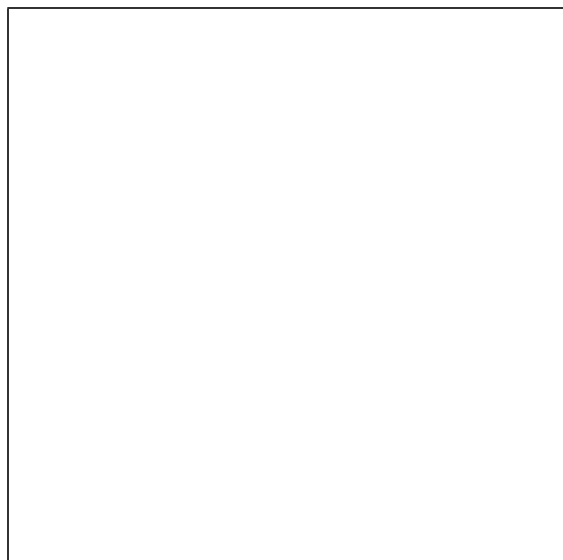
(m)  $h = 6.92$  in.



(n)  $h = 7.42$  in.

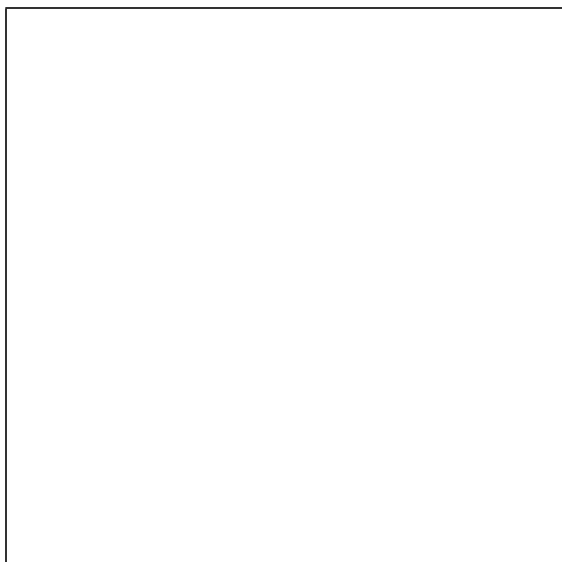


(o)  $h = 7.92$  in.

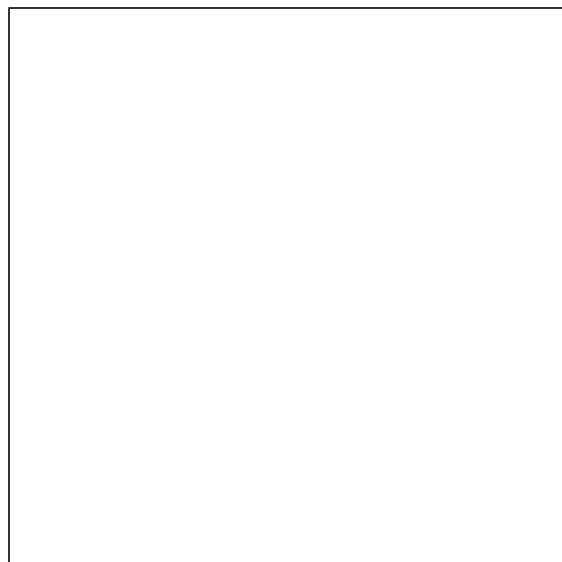


(p)  $h = 8.92$  in.

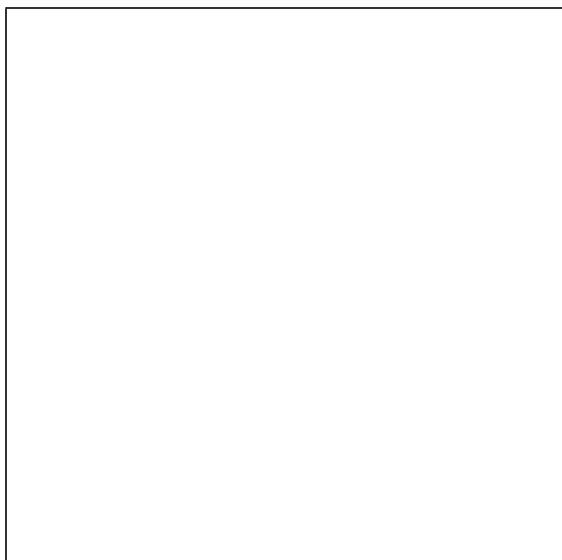
Figure A2. Concluded.



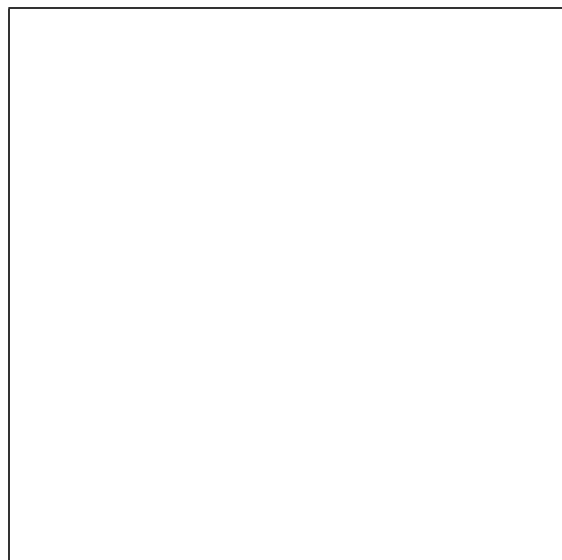
(a)  $h = 0.40$  in.



(b)  $h = 0.90$  in.

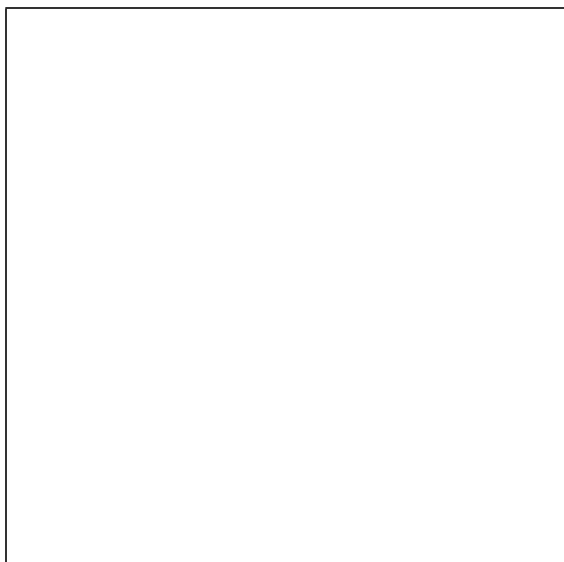


(c)  $h = 1.40$  in.

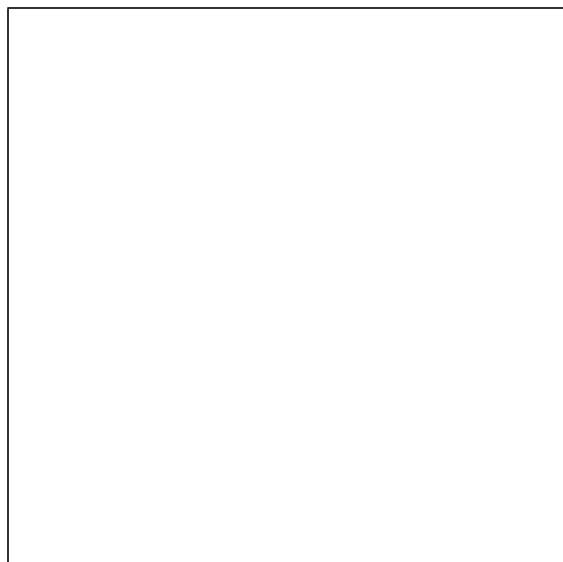


(d)  $h = 1.90$  in.

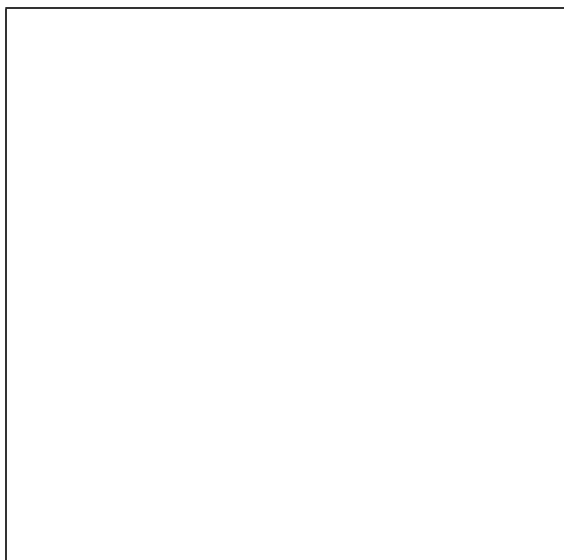
Figure A3. Schlieren photographs of roof delta at  $\alpha = 0^\circ$ . Flow is from right to left.



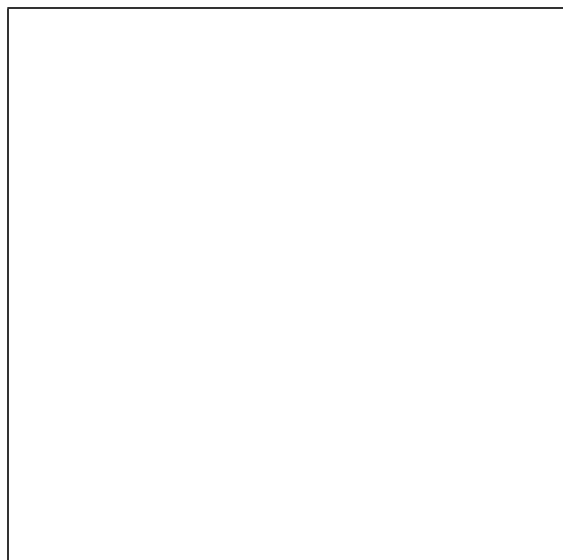
(e)  $h = 2.40$  in.



(f)  $h = 2.90$  in.

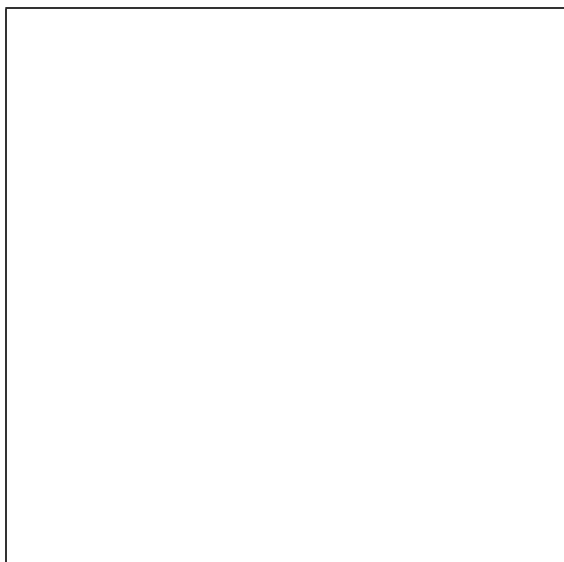


(g)  $h = 3.40$  in.

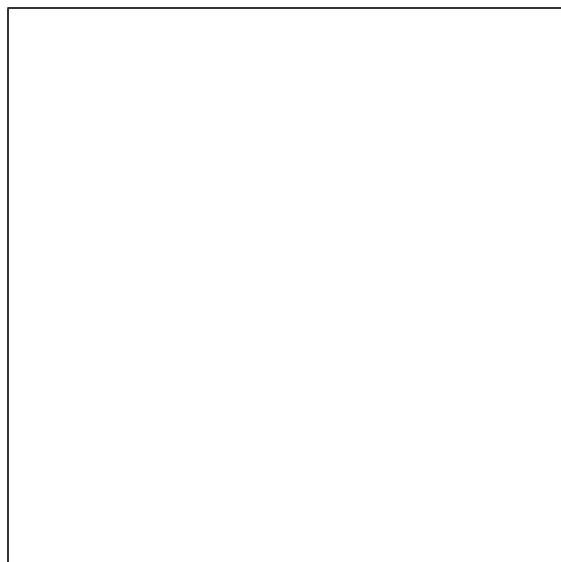


(h)  $h = 3.90$  in.

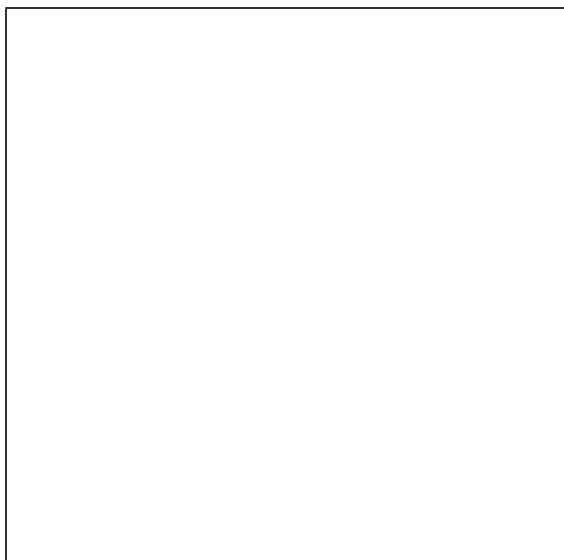
Figure A3. Continued.



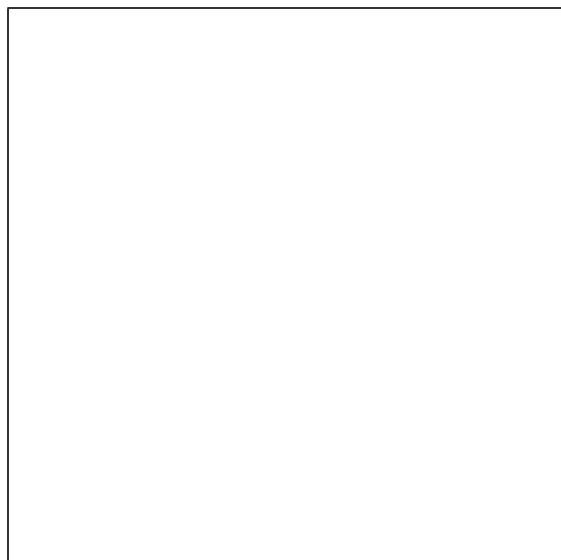
(i)  $h = 4.40$  in.



(j)  $h = 4.90$  in.



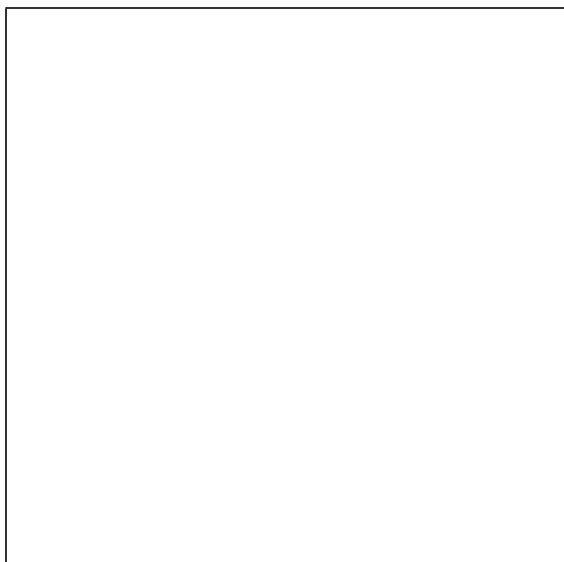
(k)  $h = 5.40$  in.



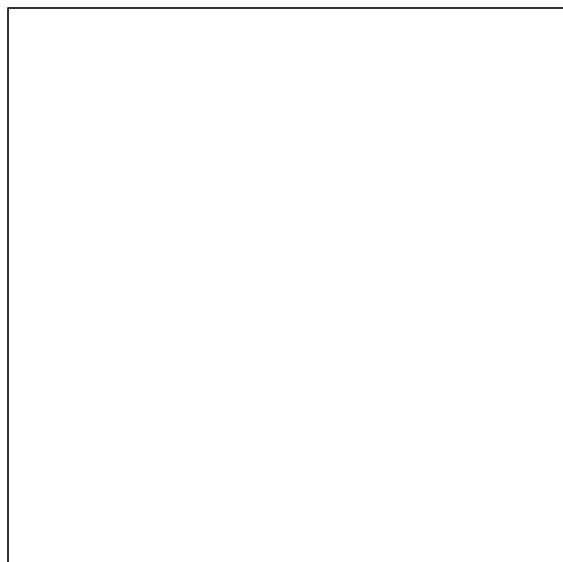
(l)  $h = 5.90$  in.

Figure A3. Continued.

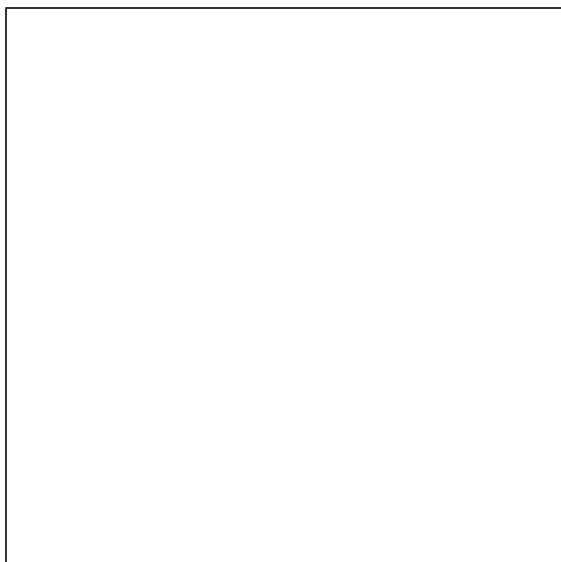




(m)  $h = 6.40$  in.

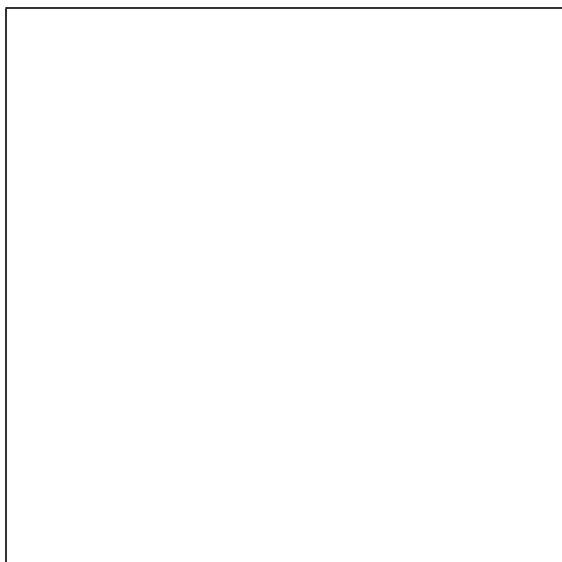


(n)  $h = 6.90$  in.

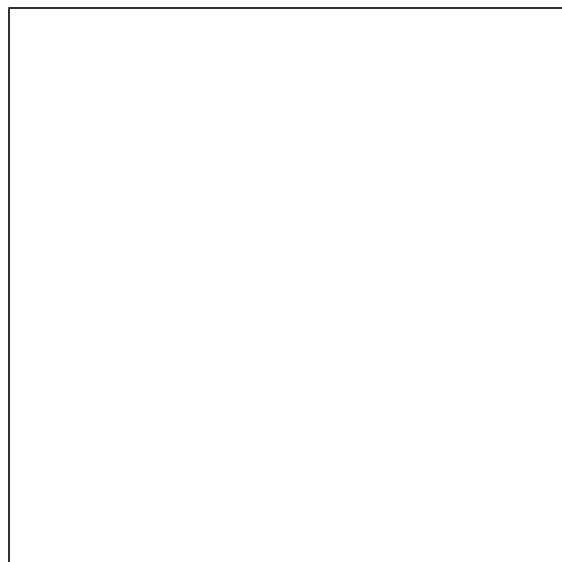


(o)  $h = 7.40$  in.

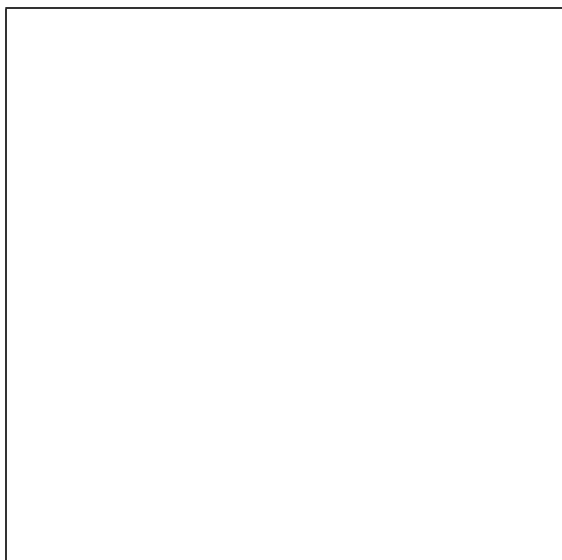
Figure A3. Concluded.



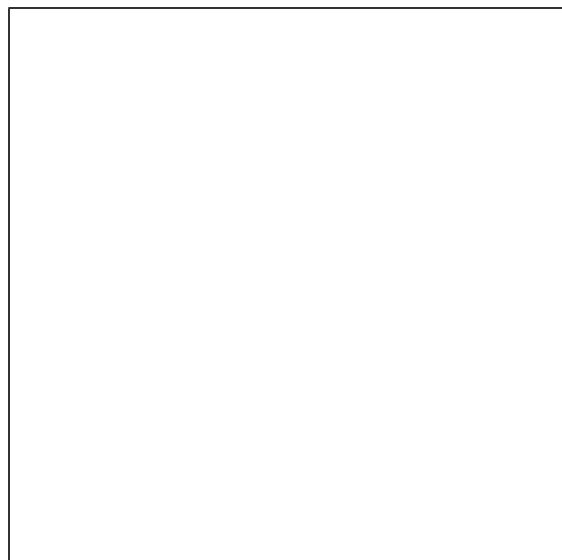
(a)  $h = 0.40$  in.



(b)  $h = 0.90$  in.

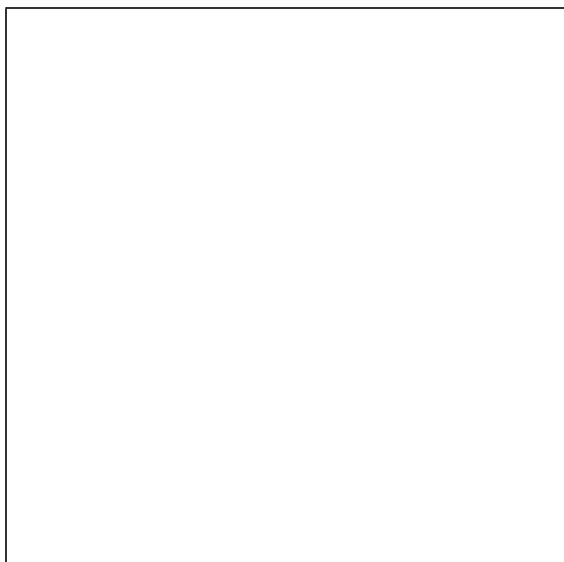


(c)  $h = 1.40$  in.

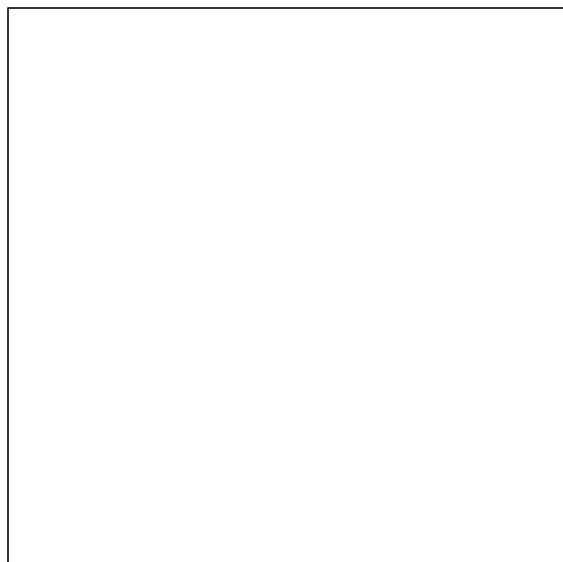


(d)  $h = 1.90$  in.

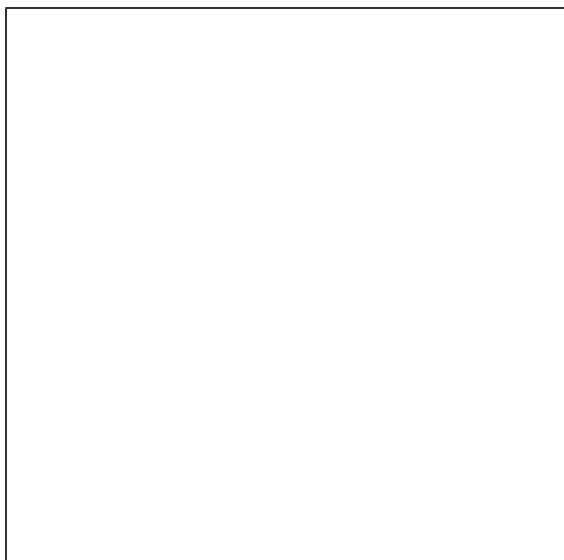
Figure A4. Schlieren photographs of roof delta at  $\alpha = 15^\circ$ . Flow is from right to left.



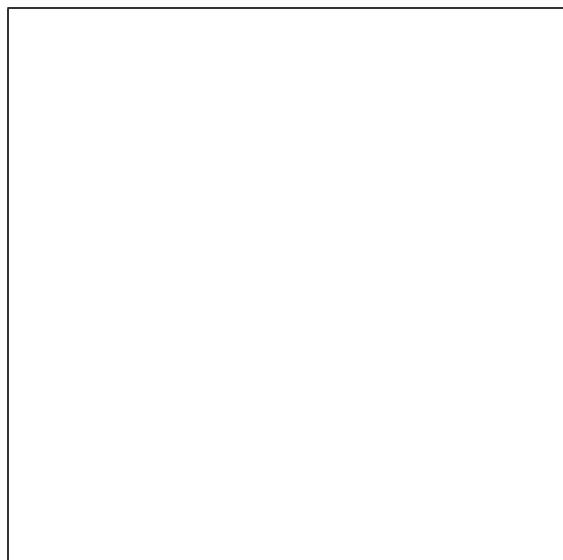
(e)  $h = 2.40$  in.



(f)  $h = 2.90$  in.

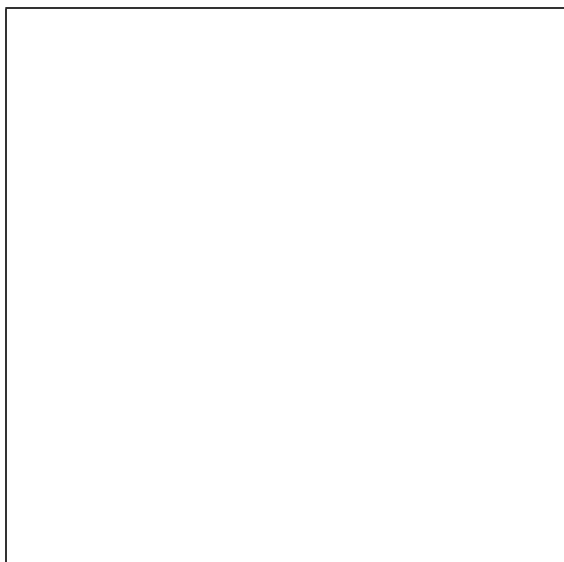


(g)  $h = 3.40$  in.

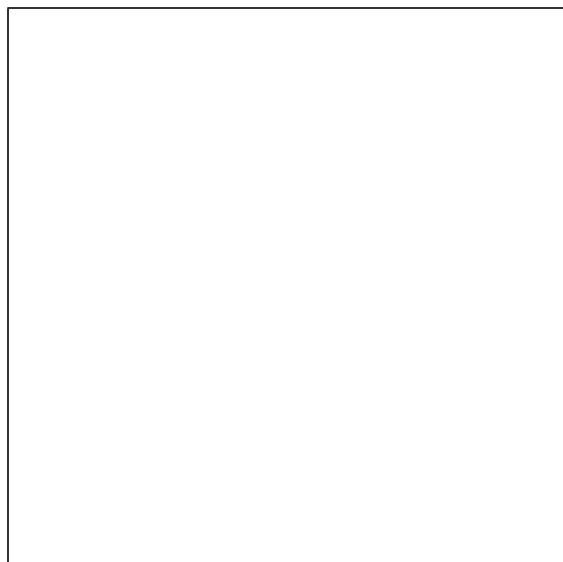


(h)  $h = 3.90$  in.

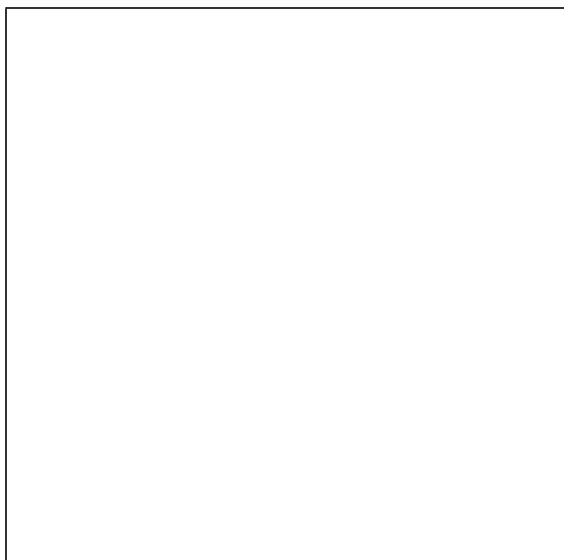
Figure A4. Continued.



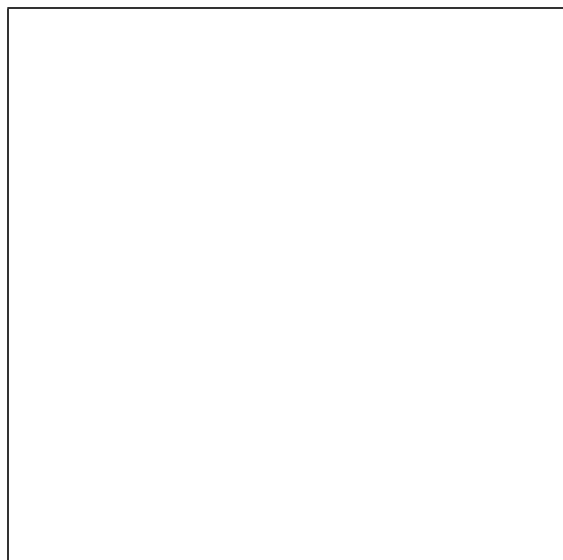
(i)  $h = 4.40$  in.



(j)  $h = 4.90$  in.

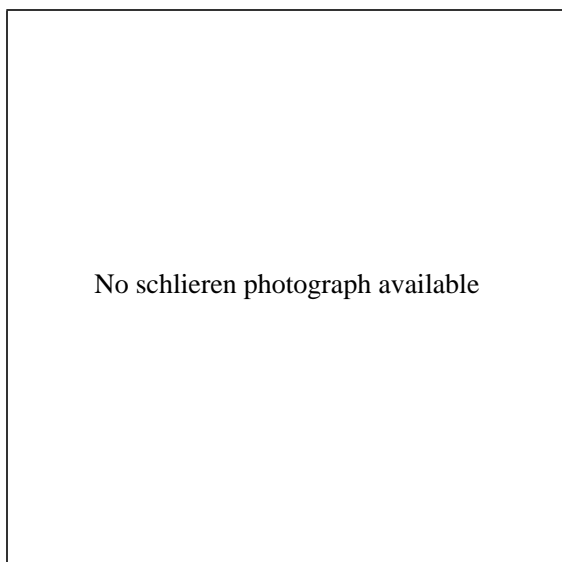


(k)  $h = 5.40$  in.

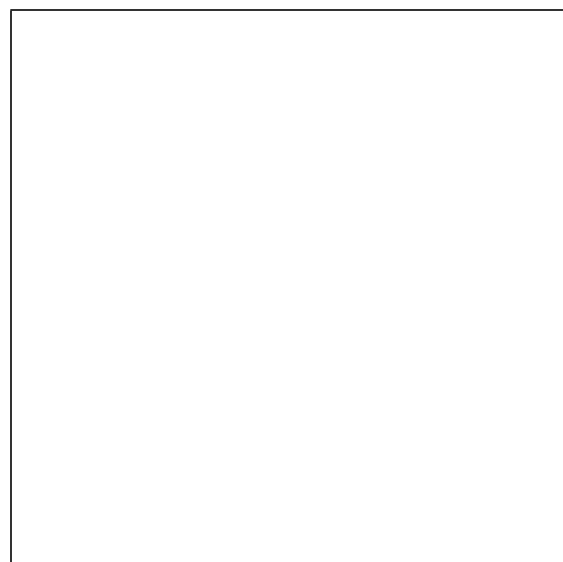


(l)  $h = 5.90$  in.

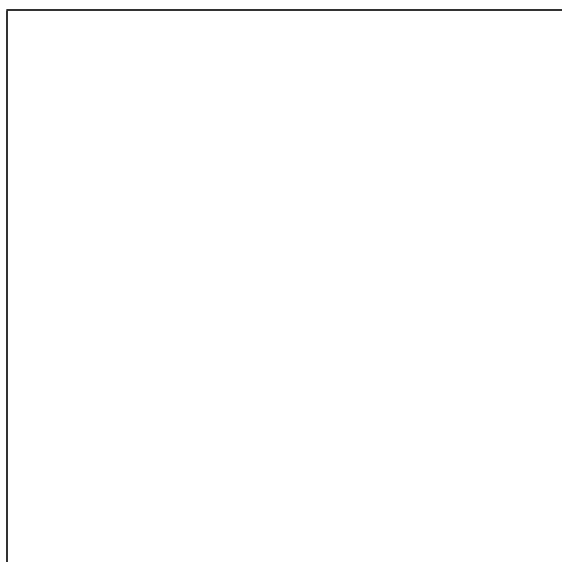
Figure A4. Continued.



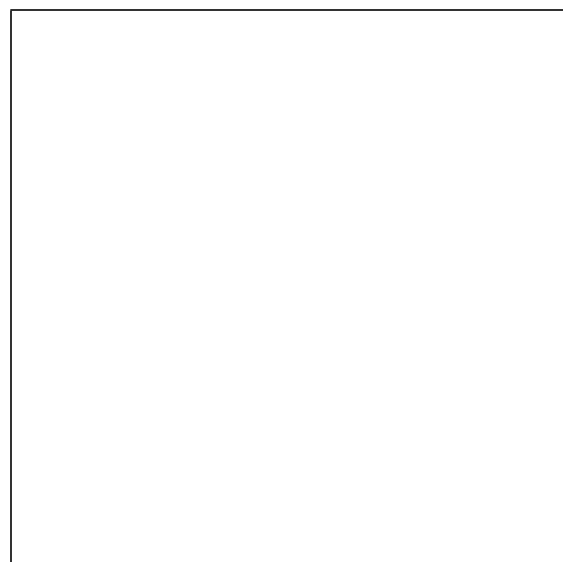
(m)  $h = 6.40$  in.



(n)  $h = 6.90$  in.

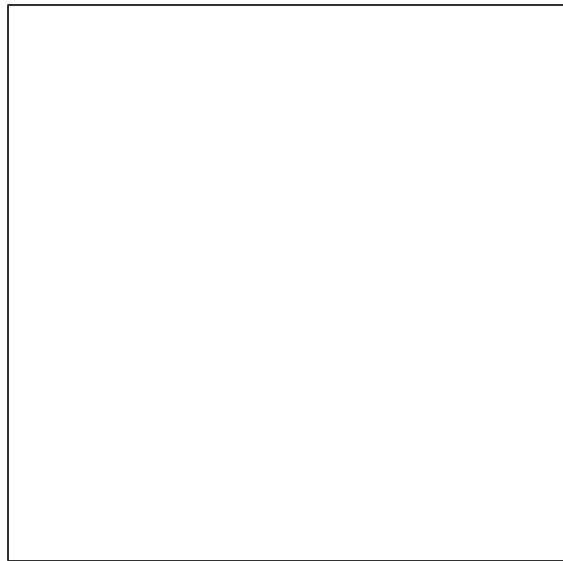


(o)  $h = 7.40$  in.



(p)  $h = 7.90$  in.

Figure A4. Continued.



(q)  $h = 8.40$  in.

Figure A4. Concluded.

REPORT DOCUMENTATION PAGE			Form Approved OMB No. 0704-0188	
Public reporting burden for this collection of information is estimated to average 1 hour per response, including the time for reviewing instructions, searching existing data sources, gathering and maintaining the data needed, and completing and reviewing the collection of information. Send comments regarding this burden estimate or any other aspect of this collection of information, including suggestions for reducing this burden, to Washington Headquarters Services, Directorate for Information Operations and Reports, 1215 Jefferson Davis Highway, Suite 1204, Arlington, VA 22202-4302, and to the Office of Management and Budget, Paperwork Reduction Project (0704-0188), Washington, DC 20503.				
1. AGENCY USE ONLY (Leave blank)		2. REPORT DATE May 1995		3. REPORT TYPE AND DATES COVERED Technical Memorandum
4. TITLE AND SUBTITLE Separation Characteristics of Generic Stores From Lee Side of an Inclined Flat Plate at Mach 6			5. FUNDING NUMBERS  WU 505-59-30-01	
6. AUTHOR(S) Floyd J. Wilcox, Jr.				
7. PERFORMING ORGANIZATION NAME(S) AND ADDRESS(ES)  NASA Langley Research Center Hampton, VA 23681-0001			8. PERFORMING ORGANIZATION REPORT NUMBER  L-17384	
9. SPONSORING/MONITORING AGENCY NAME(S) AND ADDRESS(ES)  National Aeronautics and Space Administration Washington, DC 20546-0001			10. SPONSORING/MONITORING AGENCY REPORT NUMBER  NASA TM-4652	
11. SUPPLEMENTARY NOTES				
12a. DISTRIBUTION/AVAILABILITY STATEMENT  Unclassified-Unlimited Subject Category 02 Availability: NASA CASI (301) 621-0390			12b. DISTRIBUTION CODE	
13. ABSTRACT (Maximum 200 words) An experimental investigation was conducted to determine the aerodynamic characteristics of a store as it was separated from the lee side of a flat plate inclined at 15° to the free-stream flow at Mach 6. Two store models were tested: a cone cylinder and a roof delta. Force and moment data were obtained for both stores as they were moved in 0.5-in. increments away from the flat plate lee-side separated flow region into the free-stream flow while the store angle of attack was held constant at either 0° or 15°. The results indicate that both stores had adverse separation characteristics (i.e., negative normal force and pitching moment) at an angle of attack of 0°, and the cone cylinder had favorable separation characteristics (i.e., positive normal force and pitching moment) at an angle of attack of 15°. At an angle of attack of 15°, the separation characteristics of the roof delta are indeterminate at small separation distances and favorable at greater separation distances. These characteristics are the result of the local flow inclination relative to the stores as they traversed through the flat plate lee-side flow field. In addition to plotted data, force and moment data are tabulated and schlieren photographs of the stores and flat plate are presented.				
14. SUBJECT TERMS Store separation; Hypersonics; Lee-side flows			15. NUMBER OF PAGES 44	
			16. PRICE CODE A03	
17. SECURITY CLASSIFICATION OF REPORT Unclassified	18. SECURITY CLASSIFICATION OF THIS PAGE Unclassified	19. SECURITY CLASSIFICATION OF ABSTRACT Unclassified	20. LIMITATION OF ABSTRACT	